Published in final edited form as:
Dev Biol. 2007 September 15; 309(2): 151–168. doi:10.1016/j.ydbio.2007.04.018.

Zebrafish Naked 1 and Naked 2 antagonize both canonical and non-canonical Wnt signaling

Terence J. Van Raay[a], **Robert J. Coffey**[a,b,c,†], and **Lilianna Solnica-Krezel**[d,†]

[a] Department of Medicine, Vanderbilt University Medical Center, USA

[b] Department of Cell and Developmental Biology, Vanderbilt University Medical Center, USA

[c] Department of Veterans Affairs Medical Center, Nashville, TN 37232-2279, USA

[d] Department of Biological Sciences, Vanderbilt University, Nashville, TN 37235, USA

Abstract

Wnt signaling controls a wide range of developmental processes and its aberrant regulation can lead to disease. To better understand the regulation of this pathway, we identified zebrafish homologues of Naked Cuticle (Nkd), Nkd1 and Nkd2, which have previously been shown to inhibit canonical Wnt/β-catenin signaling. Zebrafish *nkd1* expression increases substantially after the mid-blastula transition in a pattern mirroring that of activated canonical Wnt/β-catenin signaling, being expressed in both the ventrolateral blastoderm margin and also in the axial mesendoderm. In contrast, zebrafish *nkd2* is maternally and ubiquitously expressed. Overexpression of Nkd1 or Nkd2a suppressed canonical Wnt/β-catenin signaling at multiple stages of early zebrafish development and also exacerbated the cyclopia and axial mesendoderm convergence and extension (C&E) defect in the non-canonical Wnt/PCP mutant *silberblick* (*slb/wnt11*). Thus, Nkds are sufficient to antagonize both canonical and non-canonical Wnt signaling. Reducing Nkd function using antisense morpholino oligonucleotides resulted in increased expression of canonical Wnt/β-catenin target genes. Finally, reducing Nkd1 function in *slb* mutants suppressed the axial mesendoderm C&E defect. These data indicate that zebrafish Nkd1 and Nkd2 function to limit both canonical and non-canonical Wnt signaling.

Keywords

Naked Cuticle; Planar Cell Polarity; silberblick; bozozok; Wnt11; Wnt8; Dishevelled; β-catenin

Introduction

Tight regulation of the Wnt signaling pathway is a prerequisite for normal development and its misregulation has been implicated in human diseases including cancer (Clevers, 2006; Moon et al., 2004; Polakis, 2000). Wnt proteins comprise a large family of secreted, cysteine rich glycoproteins, which can activate one of three known pathways: Wnt/β-catenin (also known as canonical Wnt signaling), Wnt/Planar Cell Polarity (PCP) and Wnt/Ca^{2+}; these latter two are also collectively referred to as non-canonical Wnt signaling pathways. In vertebrates, both

†To whom correspondence should be addressed. E-mail: lilianna.solnica-krezel@vanderbilt.edu; robert.coffey@vanderbilt.edu.

canonical and non-canonical Wnt signaling start with a Wnt ligand interacting with a Frizzled receptor. This interaction, in turn, activates the intracellular protein Dishevelled (Dsh), which acts at a decisive branch point between canonical and non-canonical Wnt signaling pathways. Canonical Wnt signaling entails activation of Dsh resulting in stabilization of β-catenin, which then translocates to the nucleus where it interacts with TCF/Lef transcription factors to mediate many developmental processes such as embryonic axis specification and anterior-posterior neural patterning (for review see Cadigan and Nusse, 1997; Huelsken and Behrens, 2002; Wodarz and Nusse, 1998). Non-canonical Wnt signaling also activates Dsh and recruits it to the membrane (Park et al., 2005). Dsh, in turn, regulates the activities of proteins such as Daam1 and the small GTPases, which have been implicated in cell movement behaviors such as cell polarity, migration and intercalation during gastrulation movements of convergence and extension (C&E) (for review see Huelsken and Behrens, 2002; Jessen and Solnica-Krezel, 2005; Montcouquiol et al., 2006; Veeman et al., 2003).

During vertebrate embryogenesis the canonical Wnt/β-catenin pathway is one of the first pathways to be activated. This has been first documented in amphibian development. This pathway is activated upon fertilization when cortical rotation of the microtubule network drives β-catenin and Dsh to the pole opposite sperm entry (Miller et al., 1999; Moon and Kimelman, 1998). This rotation results in stabilization of β-catenin and activation of downstream target genes to form the dorsal gastrula organizer. Recently, Wnt11 was identified as the endogenous ligand that activates this pathway in *Xenopus laevis* (Tao et al., 2005). While there is a clear role for maternal Wnt/β-catenin signaling in establishing the gastrula organizer, there are subsequent roles for this pathway in zygotic development in both establishing and maintaining the organizer, but how this pathway is regulated during these later processes is less well understood.

One well-recognized mechanism of Wnt signaling regulation is via negative feedback inhibition and several feedback antagonists of Wnt signaling have been described including Dickopff (Dkk), Wingful/Notum, Naked, Nemo, Axin2 and β-TCRP (Chamorro et al., 2005; Giraldez et al., 2002; Gonzalez-Sancho et al., 2005; Jho et al., 2002; Niida et al., 2004; Spiegelman et al., 2000; Zeng and Verheyen, 2004). However, unlike many of the other antagonists, Naked (Nkd) can affect both canonical and non-canonical Wnt signaling. Nkd was first identified in *Drosophila melanogaster* as a Wg inducible antagonist of Wg signaling (Zeng et al., 2000) and shortly thereafter two mouse homologs, Nkd1 and Nkd2, were identified and also found to inhibit canonical Wnt/β–catenin signaling (Wharton et al., 2001; Yan et al., 2001a). It has also been established that vertebrate Nkd1 is induced by canonical Wnt/β-catenin signaling (Ishikawa et al., 2004; Schmidt et al., 2006; Yan et al., 2001a; Yan et al., 2001b).

Whereas the original *D. melanogaster nkd* mutant did not display any phenotype indicative of disrupted non-canonical Wnt/PCP signaling (Zeng et al., 2000), subsequent experiments demonstrated that Nkd overexpression can abolish Dsh activity that is specifically targeted for PCP signaling (Rousset et al., 2001). In contrast, in vertebrate models, it has been suggested that Nkds act as a switch between canonical and non-canonical Wnt/PCP signaling and that inhibition of Dsh by Nkd in canonical Wnt/β-catenin signaling results in activation of Dsh in non-canonical Wnt/PCP signaling (Yan et al., 2001a). Despite this discrepancy, the prevailing view in both vertebrates and invertebrates is that Nkd binds Dsh protein and inhibits canonical Wnt/β–catenin signaling (McEwen and Peifer, 2001; Rousset et al., 2001; Rousset et al., 2002; Wharton et al., 2001; Yan et al., 2001a; Zeng et al., 2000).

Using zebrafish as a model organism, we set out to define the role of Nkd proteins in the different stages of canonical Wnt signaling in early development. In addition, we also wanted to determine if Nkds do indeed act as a switch between canonical and non-canonical signaling or are antagonizing both pathways. Clarifying this discrepancy has important implications in

our understanding and interpretation of the control of these pathways in normal development and various disease states.

During zebrafish development, canonical Wnt/β-catenin signaling is transient and suspected to be tightly regulated. To determine how, when and where Nkds are working, it is useful to review the different stages of active canonical Wnt/β-catenin signaling during zebrafish development. The first well-known role for canonical Wnt/β-catenin signaling is in establishing the dorsal organizer (Bellipanni et al., 2006; Kelly et al., 2000). This occurs from the onset of fertilization to the 1000 cell stage, approximately 3 hours post fertilization (hpf), culminating in the initiation of transcription that is referred to as the mid-blastula transition (MBT) (Kimmel et al., 1995). We will refer to this as maternal canonical Wnt/β-catenin signaling. Induction of the homeodomain transcriptional repressor protein Bozozok (Boz) (Koos and Ho, 1998; Yamanaka et al., 1998) and the FGF antagonist MKP3 (Tsang et al., 2004) occurs during this stage. Boz, in turn, is required for the expression of the dorsal organizer markers *goosecoid* (*gsc*) and *chordin* (*chd*) (Miller-Bertoglio et al., 1997; Schulte-Merker et al., 1994a) as demonstrated by the reduction of *gsc* and *chd* expression in *boz* mutants (Fekany et al., 1999; Gonzalez et al., 2000; Shimizu et al., 2000).

Subsequently, zygotic canonical Wnt/β-catenin signaling commences at approximately 30% epiboly (5 hpf) with the expression of *wnt8* in the ventrolateral margin (Ramel and Lekven, 2004). Ventrolateral Wnt8 restricts the lateral expansion of the dorsal organizer genes *gsc* and *chd* (Erter et al., 2001; Fekany-Lee et al., 2000; Lekven et al., 2001; Ramel and Lekven, 2004). Therefore, at 50% epiboly (5.5 hpf), the dorsal expression domains of *gsc* and *chd* are a result of both the positive influence from maternal and the negative influence from zygotic canonical Wnt/β-catenin signaling (Bellipanni et al., 2006). Subsequently, from the shield stage to 60% epiboly (7.0 hpf), ventrolateral zygotic Wnt8 activity is also necessary for anterior-posterior neural patterning (Erter et al., 2001; Lekven et al., 2001). Conversely, non-canonical Wnt/PCP signaling is believed to occur only after the onset of gastrulation, demonstrated by the lack of phenotypes in most maternal-zygotic Wnt/PCP mutants in pre-gastrula embryos (Ciruna et al., 2006; Heisenberg and Nusslein-Volhard, 1997; Kilian et al., 2003; Topczewski et al., 2001).

We used gain and loss-of-function approaches to investigate the roles of Nkd1 and Nkd2 in the above Wnt-dependent processes. We found that in early zebrafish development *nkd1* and *nkd2* show distinct expression patterns. Whereas expression of *nkd1* mirrors the pattern of active canonical Wnt/β-catenin signaling, *nkd2* is expressed maternally and in a ubiquitous fashion. Further, we present data in support of the view that Nkds are necessary and sufficient to antagonize both canonical and non-canonical Wnt/PCP signaling.

MATERIALS AND METHODS

Fish maintenance

Adult zebrafish and embryos were raised at 28.5°C and were staged by anatomical criteria or hours or days post fertilization (hpf and dpf, respectively) according to Kimmel et al. (Kimmel et al., 1995). Maternal zygotic (mz) oep^{tz57}, boz^{m168} and slb^{tz215} homozygous embryos (AB* backgrounds) were collected from pairwise matings of homozygous adults. For the injection of unfertilized eggs, females were gently squeezed for eggs onto a dry petri dish and the eggs injected within 5 min. Immediately following injections, eggs were fertilized with fresh sperm diluted in Hank's Buffer (Westerfield, 1995).

Nkd cloning

Zebrafish *nkd1* and *nkd2* genes were identified in silico based on homology to murine *nkd1* and murine *nkd2*, respectively. For *nkd1* and *nkd2*, gene specific primers were designed around either the 5′UTR or the putative translational start and stop sites based on genomic sequence in the Ensembl Database. *nkd1* 5′UTR Forward primer: 5′-TTTAAATCGATCGCTGGATGTGTACGCAAG; *nkd1* ATG Forward primer: 5′-TTTAAATCGATGATGGGTAAACTTCATTCC; *nkd1* Stop Reverse primer: 5′-CATCACTTCTACCAGTCCCATCGATTAATA. *nkd2* ATG Forward primer: 5′-TTTAAATCGATGAATGGCGAAACTTCACTCCAAACATGC-3′ *nkd2* Stop Reverse primer: 5′-TTTAAATCGATGTGTCTGGTGGTAGTGGTGG-3′ Gene specific primers were adapted with a ClaI restriction enzyme sequence (included in above primer sequences) and cloned into the ClaI site of pCS2+ using standard procedures. RT-PCR was performed using SMART-RACE cDNA amplification kit (BD Bioscience) according to manufacturer's protocol from AB* shield stage embryos.

Whole-mount in situ hybridization

Staged embryos were fixed overnight at 4°C in phosphate-buffered saline solution containing 4% paraformaldehyde. In situ hybridization was carried out as described by Thisse et al. (1999). The following antisense digoxigenin-labeled probes were used: *chordin* (Miller-Bertoglio et al., 1997), *goosecoid* (Schulte-Merker et al., 1994a; Stachel et al., 1993), *no tail* (Schulte-Merker et al., 1994b), *mkp3* (Tsang et al., 2004), *six3b* (Kobayashi et al., 1998), *dlx3* (Akimenko et al., 1994), *dlC* (Haddon et al., 1998) and *nkd1* and *nkd2* (this study) and flourescein-labeled *hgg* (Inohaya et al., 1997). Probes were synthesized using T7, T3, or SP6 RNA polymerases (Ambion) and precipitated with LiCl and EtOH and resuspended in RNase free water. Probe quantity was measured by spectrophotometry and quality was assayed using gel electrophoresis.

Quantitative RT-PCR

A minimum of 20 staged embryos from at least two homozygous parents were harvested and lysed in Trizol (Gibco), snap frozen in liquid nitrogen followed by standard total RNA extraction using Phenol:Chloroform:Isoamyl Alcohol. Total RNA was digested with DNaseI prior to PCR. A total of 40ng of RNA was used per 20μL reaction. PCRs were performed on a BioRAD iCycler IQ. Sequences of primers were as follows. Nkd1 Forward: 5′-CCCAATCCCAAGCATAAG-3′; Nkd1 Reverse: 5′-CTCTCCAGGTTCTCATCC-3′; Nkd2 Forward 5′-TGGCAGGAATAGAGAACTACAC-3′; Nkd2 Reverse 5′-CCACACAGGGCTCCATAA G-3′; β-Actin Forward: 5′-TATTGTGATGGACTCTGGTGA TG-3′; β-Actin Reverse: 5′-TCGGCTGTGGTGGTGAAG-3′; 18S RNA: proprietary, ABI catalog #4333760. Each sample was run in triplicate and then averaged. Absolute quantification was determined using a standard curve generated by β-*actin* (Fig. 1) or 18S RNA (Fig. 2). Relative quantitative RT-PCR (qRT-PCR), was determined by normalizing to 1dpf.

mRNA and morpholino oligonucleotide injections

Capped mRNA was synthesized using Ambion's mMessage mMachine kit. Following transcription, the RNA was purified over a G-50 sephadex column (Roche) and diluted in RNase free water, and its quantity and quality was analyzed as described above. The RNA was diluted to a final concentration of 400ng/μL (*nkd1* and *nkd2a*), 25 ng/μL (*wnt8*) (Erter et al., 2001; Kelly et al., 1995), 10ng/μL (β-catenin), 500ng/μL (*axin* in wt), 100ng/μL (*axin* in *slb* −/−) in 1% phenol red. Two nL (*nkd1* or *nkd2a*) or 1 nL (*wnt8, β-catenin or axin*) of RNA were pressure injected into the yolk cell of one- to two-cell-stage embryos. Antisense morpholino oligonucleotides (MOs) were dissolved and diluted in water containing 1% phenol red and 0.5–8 ng were injected. At all but the 0.5 ng dose tested, there was non-specific necrosis by

mid-segmentation stages. Unless otherwise noted, 2 ng of each MO was used. The following MOs were used: *nkd1* UTR MO: 5′-ATATTTGTGAGCGTCCGTGCAGAAG-3′; *nkd1* ATG MO: 5′-GAAGTTTACCCATTTCTCTGCATCG-3′; *nkd2* splice site MO: 5′-ATGTGGGTATTAAACTGACCTGCAG-3′; *nkd2* 5′UTR MO: 5′-GCTTGTGTCAGAAGTTGTGCATCTC-3′; *nkd2* ATG MO: 5′-TGTTTGGAGTGAAGTTTCCCCATTG-3′.

Morphometric analysis of RNA expression patterns

To measure the arc of *gsc* expression at the blastoderm margin, embryos stained by whole-mount in situ hybridization were observed in the animal view under a dissecting microscope containing a 180° reticle eyepiece and the angle of *gsc* expression was measured. To measure the width of the neural plate or the position of *hgg* expression relative to the *dlx* expression domain, embryos stained by double whole-mount in situ hybridization were photographed at 25X magnification. Images were imported and measured using Image J software (NIH) as shown in Figs. 8J,K.

Measurement of Cyclopia

Live mutant embryos were scored at 2 dpf for degrees of cyclopia and the cyclopia index was determined as described by Marlow et al., (Marlow et al., 1998). Due to the variability between clutches of embryos in the penetrance and expressivity of the cyclopia phenotype in *slb* mutants (c/w Figs. 7E, 8A,G), injected embryos were directly compared to uninjected siblings. Therefore, the difference in the cyclopia index (CI) between experimental and uninjected siblings was determined for each experiment and then averaged. Unless otherwise stated, all experiments were performed in triplicate.

RESULTS

Zebrafish naked 1 and 2 have unique expression patterns

To address the roles of zebrafish Naked1 (Nkd1) and zebrafish Naked2 (Nkd2) during different stages of development, we cloned 3 homologues of the mammalian *nkd* genes. Nkd proteins contain an N-terminal myristoylation sequence, a highly conserved domain (NHR1), which also contains the conserved EF-hand that is suspected to bind Zn^{2+} (Rousset et al., 2002) and Dsh (Angers et al., 2006; Rousset et al., 2001; Rousset et al., 2002; Wharton et al., 2001), followed by a second highly homologous region (NHR2) of unknown function (Fig. 1A). The C-terminal end exhibits a conserved polyhistidine stretch of 15 and 19 amino acids that contains 80% and 79% histidines (Nkd1 and Nkd2a, respectively). Human Nkd2 also has a domain between the NHR2 and the polyhistidine tail region (TTB, Fig. 1A) that can bind TGFα and Dsh (Li et al., 2004). Zebrafish Nkd1(Genbank accession no. AY863053) is 440 amino acids (aa) in length, has 37% aa identity with zebrafish Nkd2 and 47% aa identity with human Nkd1. Nkd2 is 409 aa in length and has 46% aa identity with human NKD2. Two clones of *nkd2* were identified, *2a* (Genbank accession no. EF192161) and *2b* (Genbank accession no. EF192162), which have 18 nucleotides and 12 aa differences between them. These differences were found in multiple clones (8 clones for *nkd2a* and 5 clones for *nkd2b*) and are distributed within the exons and throughout the gene, so it is unlikely the differences are due to alternative splicing or PCR-induced errors. Currently, there is only one *nkd2* gene in the zebrafish genome database and this genomic clone contains nucleotide differences from both cDNA clones. Direct sequencing of the RT-PCR product from shield stage embryos using primers that will not discriminate between *nkd2a* and *nkd2b* showed smaller secondary peaks unique to *nkd2b* suggesting that *nkd2a* is the predominant species. We interpret this data to mean that two *nkd2* genes are likely present in the zebrafish genome, which will need to be verified by further analysis. Preliminary analysis suggests that there are no functional differences between proteins encoded by them and this study used *nkd2a* exclusively.

Whole-mount in situ hybridization analysis revealed that expression of *nkd1* begins after the mid-blastula transition (MBT) at dome stage in the putative dorsal organizer region (Fig. 1C) and at 50% epiboly is robust along the blastoderm margin (Fig. 1D). At shield stage, expression has cleared out of the shield within the superficial epiblast layer but is turned on again in the internalized axial mesendoderm (Figs. 1E,F). This became more prominent at 75% epiboly as expression was observed in the axial mesendoderm as well as along the entire blastoderm margin (Figs. 1G,H). At tailbud stages (Fig. 1I), expression was observed in the mid-hindbrain boundary (mhb), paraxial mesoderm, adaxial cells and was absent from the developing posterior neural tube (data not shown). During segmentation stages, expression continued in the anterior CNS, similar to tailbud stages and was observed in the developing somites and in the tailbud (Figs. 1J). At the 10 somite stage, there was robust expression in the mhb, hindbrain, anterior neural tube, developing somites, adaxial cells and in the presomitic mesoderm (Fig. 1K). At 1 dpf, expression continued in the eye, mhb, rhombomeres, somites, neural tube and developing tail (Fig. 1L). We did not detect expression of *nkd1* pre-MBT by whole-mount in situ hybridization (Fig. 1B). In contrast, expression of *nkd2* is maternal and ubiquitous (Figs. 1M–Q) until 1 dpf when *nkd2* expression becomes confined to the anterior CNS with slight expression in the developing tail (Fig. 1R). Interestingly, expression of *nkd1*, but not *nkd2*, coincides with sites of active zygotic canonical Wnt/β-catenin signaling (Dorsky et al., 2002), which is consistent with its reported role as a feedback antagonist.

To quantify the levels of *nkd1* RNA, qRT-PCR was performed at several key stages in development. We found that the qRT-PCR data supports the in situ expression profile of *nkd1* with one key difference. qRT-PCR was able to detect the presence of *nkd1* in 16 cell stage embryos, although the levels were very low (Fig. 1S). Also in agreement with the in situ data, qRT-PCR analysis showed that *nkd1* expression rises by dome stage and increases at shield stage, before receding at 1 dpf. The detection of pre-MBT *nkd1* expression by qRT-PCR leaves open the possibility that there is maternal *nkd1* expression, although at very low levels. For quantitative purposes, levels were normalized to 1dpf.

Nkd1 expression is a target of canonical Wnt/β-catenin signaling

The expression of *nkd1* suggests that it is a target of canonical Wnt/β-catenin signaling. To test this, we overexpressed a constitutively active form of *β-catenin*, which has an N-terminal truncation making it resistant to degradation (Yost et al., 1996), and assayed for ectopic *nkd1* expression. As predicted, at dome stage, we observed robust ectopic *nkd1* expression (Fig. 2B), whereas endogenous *nkd1* expression was just starting to be detected (Fig. 2A). Conversely, when we inhibited canonical Wnt/β-catenin signaling by overexpression of *axin* RNA, a decrease in *nkd1* expression at 50% epiboly in the blastoderm margin was observed (Fig. 2D). Together, these data suggest that *nkd1* expression is positively regulated by canonical Wnt/β-catenin signaling.

To further test this hypothesis, we analyzed the expression of *nkd1* in different genetic backgrounds that have perturbed canonical Wnt/β-catenin signaling. The zebrafish homeobox gene *boz* is a direct target of maternal Wnt/β-catenin signaling (Bellipanni et al., 2006; Shimizu et al., 2000) and is required for the formation of the gastrula organizer and specification of dorsoanterior structures (Fekany et al., 1999). *boz* mutants have defects in the development of axial structures (Fekany et al., 1999) due to ectopic Wnt8 activity in the dorsal blastoderm margin (Erter et al., 2001; Fekany-Lee et al., 2000). Therefore, Boz is necessary for the induction of organizer genes and subsequently for the restriction of mediolateral Wnt8 from the dorsal blastoderm. If *nkd1* is a target of canonical Wnt/β-catenin signaling through Boz, then we would predict that *nkd1* RNA levels would be decreased at dome stage in *boz* mutants, similar to the expression of *gsc* in *boz* mutants (Fekany et al., 1999). Indeed, we observed an absence of *nkd1* expression in *boz* mutants in the putative organizer region (Fig. 2F). To confirm

this, we performed qRT-PCR on dome stage wild-type and homozygous *boz* embryos. Consistent with the in situ data, we observed a significant decrease in *nkd1* expression at dome stage in *boz* embryos (Fig. 2M) ($p < 0.01$). In contrast, at shield stage, we would predict an increase in *nkd1* expression in *boz* mutants, due to ectopic Wnt8 signaling in the dorsal midline (Fekany-Lee et al., 2000). Accordingly, at shield stage we observed a increase in *nkd1* expression in the organizer region of *boz* mutants, which was also confirmed by qRT-PCR (Figs. 2J,M) ($p < 0.001$). To further explore the regulation of *nkd1*, we examined the expression of *nkd1* in maternal zygotic *one-eyed pinhead* (mz*oep*) mutants, which lack dorsolateral mesoderm and are defective in Nodal signaling (Gritsman et al., 1999). Previously, we demonstrated that Nodal-deficient embryos have reduced *wnt8* expression juxtaposed to the dorsal organizer region (Erter et al., 2001). Therefore, we would predict a similar reduction in *nkd1* expression in mz*oep* mutants as a consequence of reduced *wnt8* expression. As predicted, we observed a decrease in *nkd1* expression at shield stage, specifically in the dorsal region where it was completely absent (Fig. 2K). We did not find any alterations in *nkd1* expression at dome stage, suggesting that induction of *nkd1* expression is normal but the maintenance of *nkd1* expression in the dorsal region is perturbed in mz*oep* mutants. These results provide further support for the notion that *nkd1* expression is positively regulated by canonical Wnt/β-catenin signaling.

To determine if *nkd1* expression is also regulated by non-canonical Wnt/PCP signaling, we performed a similar analysis in maternal zygotic *silberblick* (mz*slb*) embryos in which the *wnt11* gene is inactivated (Heisenberg et al., 2000). We found no difference in *nkd1* expression at dome, shield, or 2–3 somite stages, when compared to wild-type embryos (Figs. 2H,L and not shown). Therefore, we conclude that *nkd1* expression is not under the influence of Wnt11, and by extrapolation, non-canonical Wnt/PCP signaling. Taken together, this data supports the hypothesis that *nkd1* is positively regulated by canonical Wnt/β-catenin signaling.

Nkds can antagonize Wnt/β–catenin signaling during dorsoventral patterning

Previous reports have demonstrated that Nkds act as negative regulators of canonical Wnt/β-catenin signaling (Wharton et al., 2001; Yan et al., 2001a; Zeng et al., 2000). To determine if Nkd1 and Nkd2a can antagonize maternal Wnt/β–catenin signaling, we injected synthetic *nkd1* or *nkd2a* RNA into zygotes within 7 min of fertilization to maximize the effectiveness of targeting maternal Wnt/β-catenin signaling. We then assayed at sphere stage (4.0 hpf) for expression of *mkp3*, which initially is a direct target of maternal Wnt/β–catenin signaling (Tsang et al., 2004). Injection of *nkd1* or *nkd2a* resulted in 51% (n=92) and 55% (n=76) of embryos having reduced *mkp3* expression, respectively (Figs. 3B,L). Similar results were obtained with *boz* probe (*nkd1*: 23% reduced, n=39; *nkd2a*: 72% reduced, n=33, data not shown). This is consistent with the notion that both Nkd1 and Nkd2 can antagonize maternal Wnt/β–catenin signaling that promotes organizer formation (Kelly et al., 2000). At 50% epiboly, the arc of dorsal *gsc* and *chd* expression has been fine tuned by the positive influence of maternal and the negative influence of ventrolateral zygotic Wnt/β–catenin signaling. Analysis of *gsc* expression at 50% epiboly in embryos injected within 7 min of fertilization with *nkd1* or *nkd2a* RNA displayed mixed results: 9% (*nkd1*; n=110) and 9% (*nkd2a*; n=70) showed reduced *gsc* expression (asterisks Fig. 3D). However, in the same experiment, 80% (*nkd*1) and 50% (*nkd2a*) of injected embryos showed expanded *gsc* expression (arrowhead Fig. 3D) when compared to uninjected controls (Fig. 3C). We observed similar results using *chd* probe (*nkd1*: 7% reduced, 52% expanded, n=27; *nkd2a*: 21% reduced, 21% expanded, n=19; data not shown). We interpret these results to mean that overexpression of Nkd1 or Nkd2a can interfere with both maternal and zygotic Wnt/β–catenin signaling, affecting both the positive and negative influences of canonical Wnt/β-catenin signaling on the organizer gene expression.

To determine if we could more effectively target maternal Wnt/β-catenin signaling, and therefore obtain more significant reduction of *gsc* expression at 50% epiboly, we injected *nkd1* or *nkd2a* RNA into unfertilized eggs followed by in vitro fertilization. This resulted in 27% of *nkd1* and 26% of *nkd2a* RNA injected embryos exhibiting reduced *gsc* expression with 54% and 53% of *nkd1* and *nkd2a* injected embryos having expanded *gsc* expression, respectively (*nkd1*: n=26; *nkd2a*: n=19; data not shown). This data argues that Nkd1 and Nkd2a are capable of antagonizing maternal Wnt/β–catenin signaling involved in organizer formation. These results are summarized in Fig. 5B.

As *nkd2* is maternally expressed, we hypothesized that Nkd2 is the principal protein to restrict maternal Wnt/β–catenin signaling. To test this, we designed antisense morpholino oligonucleotides (MO) targeted to either the 5′UTR or the ATG transcriptional start site of *nkd2* both of which recognize *nkd2a* and *nkd2b* and thus repress translation of all maternal *nkd2* RNA. In addition, we designed a MO targeted to a *nkd2* splice site, which should prevent splicing of zygotic but not maternal *nkd2* RNA. Injection of either the *nkd2* 5′UTR or the *nkd2* ATG MO resulted in a modest but consistent expansion of the *mkp3* expression domain in 50% of injected embryos at sphere stage (Figs. 3E,L) (n=165). As a control, injection of a *nkd2* MO targeted to a *nkd2* splice site resulted in embryos of which only 7% showed reduced, and 7% showed expanded *mkp3* expression, and which was not significantly different from uninjected controls (Figs. 3F,L) (n=45). Efficacy of the MOs were confirmed by Western blot analysis using anti-myc antibodies and C-terminal myc-tagged Nkd1 and Nkd2 proteins (ATG and UTR MOs) or by RT-PCR (Nkd2 Splice MO) (data not shown).

We next assayed for *gsc* expression at 30% epiboly in Nkd2 MO injected embryos. At this stage, ventrolateral *wnt8* expression is being initiated (Kelly et al., 1995; Ramel and Lekven, 2004) and so it is unlikely that endogenous Wnt8 signaling will have had sufficient time to adversely affect *gsc* expression at 30% epiboly. In agreement with the *mkp3* expression data, we observed a significant increase in the arc of *gsc* expression compared to uninjected controls (Figs. 3I,K; uninj = 67.4° ±7.6 n=27; *nkd2* MO = 79.1° ± 13.3, n=29; $p<0.001$). The expansion of *mkp3* and *gsc* expression in Nkd2 knockdown embryos argues that Nkd2 is necessary for restricting maternal Wnt/β–catenin signaling involved in organizer formation. These results are summarized in Fig. 5C.

Our in situ analysis did not detect maternal *nkd1* expression, but the more sensitive qRT-PCR analysis detected low levels of *nkd1* RNA in 16-cell stage embryos. Therefore, we wanted to determine if this low level was sufficient to antagonize maternal Wnt/β-catenin signaling. We found that injection of *nkd1* MO targeting the ATG start site did not affect the size of *mkp3* expression at sphere stage (n=34, data not shown). From this analysis, we conclude that the low level of maternal *nkd1* RNA detected by qRT-PCR does not significantly contribute to the antagonism of maternal Wnt/β-catenin signaling. However, significant zygotic expression of *nkd1* in the putative dorsal region commences at dome stage (Fig. 1C), after the onset of *mkp3* expression (Tsang et al., 2004) (data not shown). Thus, it is possible that Nkd1 may also antagonize or restrict maternal Wnt/β–catenin signaling that contributes to the establishment of the organizer, but a stage later than Nkd2. To test this, we injected *nkd1* MOs in a standard 1 cell injection and assayed for *gsc* expression at 30% epiboly. Interestingly, we observed a modest, but significant, increase in the arc of *gsc* expression (Figs. 3H,K) (*nkd1* MO = 73.3° ± 12.2, n=43; $p<0.05$). To see if there is an additive or synergistic effect between the inhibition of Nkd1 and Nkd2, we co-injected MOs designed to target both genes and performed a similar assay. We observed an additive increase in the arc of *gsc* expression that was significantly different from *nkd2* MO embryos injected with *nkd2* MO alone (Fig. 3J,K) (*nkd1+nkd2* MO = 81.2° ± 16.3 n=25; $p< 0.01$) and from uninjected controls ($p<0.0001$). This data supports our hypothesis that Nkd1 is also necessary to limit maternal Wnt/β-catenin signaling involved in organizer formation.

Nkd1 and Nkd2 can alter medio-lateral Wnt8 Activity

Thus far, we have determined that early overexpression of Nkd1 or Nkd2a can antagonize maternal and zygotic Wnt/β-catenin. To further determine if Nkd1 and Nkd2a do indeed act as repressors of zygotic Wnt/β-catenin signaling, we performed standard 1–2 cell overexpression assays and analyzed the expression of the dorsal marker *gsc* at 50% epiboly. As these are later injections than described above, we never observed embryos with reduced *gsc* expression and so expansion of the *gsc* domain in these experiments was interpreted as a result of inhibition of zygotic, mediolateral Wnt8 signaling (Fig. 5D). Indeed, injection of *nkd1* or *nkd2a* at the 1–2 cell stage resulted in a highly significant increase of approximately 50% in mediolateral *gsc* expression at 50% epiboly (Figs. 4A,B) (uninj = 56.1° ±13.5 n=74; *nkd1* =84.7° ±19.5 n=17; p<0.0001; *nkd2a* = 84.4° ± 13.7, n=17; p<0.0001). These results are summarized in Fig. 5D. Interestingly, this increase in dorsal gene expression at blastula stages did not translate into a dorsalized embryo at 1 dpf and doses of *nkd1* or *nkd2a* RNA as high as 2.4 ng had little observable effect on morphology at 1 dpf (data not shown).

As described above, reducing both Nkd1 and Nkd2 protein levels expands the organizer at 30% epiboly (Figs. 3J,K). However, analysis of *gsc* expression at 50% epiboly in *nkd1* MO+ *nkd2* MO co-injected embryos showed that the arc of *gsc* expression was dramatically smaller compared to 30% epiboly and comparable to uninjected controls (Fig. 4D) (*nkd1*+ *nkd2* Mo =56.8.7° ±11.3 n=39, p=0.77). This phenomenon likely demonstrates the combined effects of the early positive and subsequent negative influence of Wnt/β-catenin signaling on the size of the organizer. With reduced Nkd antagonism, there is an increase in maternal canonical Wnt/β-catenin signaling that results in an expanded organizer. This is counteracted by the subsequent increase in the zygotic, lateral Wnt8 activity, which restricts lateral organizer expansion. It is also interesting to note that while knockdown of Nkd1 or Nkd2 resulted in an expansion of *gsc* expression at 30% epiboly (Figs. 3H,I,K, 5C), overexpression of *nkd1* or *nkd2a* RNA also resulted in an expansion of *gsc* expression, but at 50% epiboly, approximately 1 hr later (Figs. 4B, 5D). While these are seemingly incongruent results, we argue that the *nkd* MO injections expand the positive influence of maternal Wnt/β-catenin signaling on organizer formation (increase in arc of *gsc* expression at 30% epiboly), while the overexpression at the 1–2 cell stage predominantly reduces the negative influence of zygotic, ventrolateral Wnt/β-catenin signaling on organizer maintenance (increase in the arc of *gsc* expression at 50% epiboly). Thus, one would predict that co-injection of *nkd1* or *nkd2a* RNA at the 1–2 cell stage along with *nkd1* and *nkd2* MOs should result in an additive effect on the size of *gsc* expression at 50% epiboly. Indeed, co-injection of *nkd1* and *nkd2* MOs that do not target the synthetic RNA of *nkd1* or *nkd2a* resulted in a dramatic and significant increase in the arc of *gsc* expression compared to RNA or MOs injected separately (Figs. 4C,D) (*nkd1* UTR MO + *nkd2* UTR MO + *nkd1* RNA = 103° ± 20.0, n=45; p<0.01; *nkd1* UTR MO + *nkd2* UTR MOs + *nkd2a* RNA = 96.1° ± 21.5, n=45; p<0.05). These results are summarized in Fig. 5E.

Nkd1 and Nkd2a can inhibit ventralizing and posteriorizing activity of Wnt8

To pursue the role of Nkd1 *and* Nkd2 as canonical Wnt antagonists further, we tested the ability of Nkd1 *and* Nkd2 to modulate the effects of excess Wnt8. A low dose of *wnt8* RNA in a standard 1–2 cell injection mildly increased the size of *gsc* expression in the dorsal organizer (Fig. 4D) (*wnt8* = 65.8° ± 15.9, n=30; p<0.01) but this dose can profoundly affect the anterior-posterior patterning of the embryo resulting in posteriorization of the forebrain characterized by an eyeless phenotype (Figs. 6A,C) (Erter et al., 2001;Lekven et al., 2001). Co-injection of *wnt8* with *nkd1* or *nkd2a* resulted in a near complete suppression of the eyeless phenotype (Figs. 6B,C), consistent with the role of Nkd proteins as canonical Wnt antagonists (*wnt8*: n= 432; *wnt8*+*nkd1* n=148, p<0.0001; *wnt8*+*nkd2a* n=141; p<0.0001).

The zebrafish homeobox gene *boz* is required for the formation of the gastrula organizer and specification of dorsoanterior structures and *boz* mutants have defects in the development of axial structures (Fekany et al., 1999). This is due to ectopic Wnt8 activity in the dorsal blastoderm margin that results in axial mesoderm deficiency (Fekany-Lee et al., 2000). Therefore, we wanted to determine if Nkds could counteract ectopic, but physiological, levels of Wnt8 in this mutant. Injections of *nkd1* or *nkd2a* into *boz* mutants at the 1 cell stage suppressed axial deficiencies as revealed by the expression of the notochord marker *notail* (*ntl*) (Figs. 6D,E) (*boz* uninj: 11% with complete *ntl* expression n=27; *boz* + *nkd1:* 96% with complete *ntl* expression n= 24; *boz* + *nkd2a:* 52% with complete *ntl* expression, n=25) and by the morphological presence of a notochord at 1 dpf (Figs. 6F,G) providing evidence that Nkd1 and Nkd2 are sufficient to antagonize physiological levels of ectopic Wnt8.

To determine if Nkd1 and Nkd2 influence canonical Wnt/β-catenin signaling by acting upstream or downstream of β-catenin, we co-injected *β-catenin* RNA along with *nkd1 or nkd2a* RNA or *β-catenin* RNA alone and assayed for ectopic *gsc* expression at 50% epiboly and for dorsalized phenotypes at 1 dpf. As expected, excess Nkd1or Nkd2 were unable to suppress the effect of ectopic β-catenin at either the molecular (n=30, data not shown) or morphological level (n=46, data not shown) arguing that Nkd1 and Nkd2 function downstream of Wnt ligands but upstream of β-catenin.

Nkds can inhibit non-canonical Wnt signaling

The results described above support the notion that Nkd1 and Nkd2 are both necessary and sufficient for antagonizing canonical Wnt/β–catenin signaling. As Nkds have been shown to bind Dsh (Angers et al., 2006; Li et al., 2004; Rousset et al., 2001; Rousset et al., 2002; Wharton et al., 2001; Yan et al., 2001a), which acts at a critical node between canonical and non-canonical Wnt signaling, we next wanted to determine if Nkds can also effectively regulate non-canonical Wnt signaling. To accomplish this, we took advantage of the *silberblick*/Wnt11 (*slb*) mutant which has impaired C&E movements during gastrulation and abnormal extension of axial tissues resulting in cyclopia (Heisenberg et al., 2000). This phenotype can effectively be suppressed by injection of synthetic *wnt11* RNA (Heisenberg et al., 2000) or exacerbated by additional mutations or alterations in the non-canonical Wnt/PCP pathway (Kilian et al., 2003; Marlow et al., 1998; Topczewski et al., 2001; Westfall et al., 2003). To test how Nkd1 and Nkd2a might affect the *slb* phenotype, we injected *nkd1 or nkd2a* RNA into *slb* embryos and assayed for C&E of axial mesoderm at 2–3 somites and the presence of cyclopia at 2 dpf. Overexpression of *nkd1* or *nkd2a* RNA in *slb* mutants exacerbated the *slb* phenotype consistently resulting in embryos with increased cyclopia (Fig. 7C). The Cyclopia Index (CI) (Marlow et al., 1998) was used to quantify the penetrance and expressivity of cyclopia, where CI = I represents normal eye spacing as in wild type, CI = II–III is mild to moderate synopthalmia and CI = IV–V is severe synopthalmia to complete cyclopia, respectively (Figs. 7A–C). While there was some variability between clutches of embryos, we found that uninjected *slb* embryos had an average CI of 2.80 ± 0.46 (n=290). However, injection of *nkd1* or *nkd2a* synthetic RNA into *slb* embryos resulted in a shift towards more severe cyclopia. For *nkd1* injected *slb* embryos, the CI increased by 0.97 to an average of 3.77 (n=134) while for *nkd2a* injected *slb* embryos the CI increased by 0.28 to an average of 3.08 (n=73). In contrast, injection of synthetic *wnt11* RNA into *slb* embryos decreased the penetrance and expressivity of cyclopia with a reduction in the CI by 1.69 to an average of 1.11 (n=146) relative to uninjected mutant siblings. This argues that Nkd1 and Nkd2a can inhibit non-canonical Wnt/PCP signaling.

To analyze further the effect of Nkds on C&E in *slb* mutants, we looked at the relative position of molecular marker expression boundaries at early somitogenesis when the *slb* phenotype is strongest (Heisenberg et al., 2000). The axial mesoderm marker *hgg* defines the position of the

most anterior prechordal mesoderm (Inohaya et al., 1997), relative to the neuroectoderm and non-neural ectoderm boundary demarcated by the expression of *dlx3* (Akimenko et al., 1994). In wild-type embryos, due to C&E movements, the *hgg* expression domain is wholly anterior to the *dlx3* expression domain (Figs. 7D,I). By contrast, in the majority of uninjected *slb* embryos (72%, n=107), defects in the extension of the axial mesendoderm result in the *hgg* expression domain underlying the *dlx3* expression domain (Figs. 7E,I) (Heisenberg et al., 2000). In *slb* embryos injected with *nkd1* or *nkd2a* RNA, the posterior shift of the *hgg* expression domain was exacerbated in 25% of mutant embryos (Figs. 7G,I), arguing that Nkd1 and Nkd2a overexpression interferes with non-canonical Wnt/PCP signaling. In a separate assay, we tested whether and how Nkd1 or Nkd2a could influence the ability of Wnt11 to rescue the *slb* mutant phenotype. Injection of synthetic *wnt11* RNA into *slb* mutants resulted in the near complete rescue of cyclopia (data not shown) and the extension of the axial mesendoderm defect (Figs. 7F,I) as previously reported (Heisenberg et al., 2000). However, co-injection of *wnt11* with *nkd1* or *nkd2a* RNAs into *slb* embryos resulted in a phenotype similar to *slb* embryos injected with *nkd1* or *nkd2a* RNA alone (Figs. 7H,I), suggesting that Nkds can effectively block the activity of non-canonical Wnt signaling.

The effect of overexpression of Nkds on the position of the prechordal plate in *slb* mutants, and the expression of *nkd1* in the axial mesendoderm at 75% epiboly (Fig. 1G), suggests that Nkd1 may have a role in non-canonical Wnt/PCP signaling in the C&E of axial mesendoderm. Indeed, injection of *nkd1* MO into *slb* mutant embryos resulted in the partial suppression of the axial mesendoderm extension defect (Fig. 8B). To quantify this, we measured the percentage of embryos in which the prechordal plate was positioned anterior to the overlying neuroectoderm (Fig. 8J). While uninjected *slb* controls had an average of 68.7% of the prechordal plate lying anterior to the overlying neuroectoderm, this increased to 81.8% when Nkd1 activity was reduced (Fig. 8J) ($p<0.001$). However, there was no significant difference in the width of the neural plate (Figs. 8B,K) arguing that Nkd1 is required for antagonizing Wnt11 in the extension of axial mesendoderm, but not for convergence of the neuroectoderm. As *nkd2* has ubiquitous expression, we also tested if the *nkd2* MO had a similar effect. Surprisingly, we found that the injection of *nkd2* MO into *slb* mutant embryos resulted in an exacerbated phenotype compared to uninjected *slb* controls (Fig. 8C). In *nkd2* MO injected mutants, on average, only 59.1% of the prechordal plate was lying anterior to the overlying neuroectoderm, which was significantly different from uninjected mutant siblings (Fig. 8J) ($p<0.05$), and the width of the neural plate was significantly wider (Fig. 8K) ($p<0.0001$). This argues that Nkd2 is necessary for the proper extension of axial mesendoderm and convergence of the neural ectoderm, but in a manner that is different from Nkd1.

Our studies indicate that reducing Nkd1 function can enhance both canonical Wnt/β-catenin and non-canonical Wnt/PCP signaling. However, as non-canonical Wnt/PCP signaling is believed to occur after maternal and zygotic canonical Wnt/β-catenin signaling and that *nkd1* expression is a target of the canonical pathway, the effect of Nkd1 on non-canonical Wnt/PCP signaling could be an indirect effect. To test this hypothesis, we significantly reduced canonical Wntβ-catenin signaling in *slb* embryos and assayed for effects on non-canonical Wnt/PCP signaling with and without *nkd1* MO. Injection of *axin* RNA, which is a critical component of the canonical Wnt/β-catenin destruction complex, into *slb* embryos resulted in a predicted and significant decrease in the arc of *gsc* expression at 50% epiboly compared to uninjected controls (Figs. 8D,E,L) (Uninj = 76.7° ± 11.5, n=13; *axin* = 49.2° ± 13.6, n=25; $p<0.001$). Co-injection of *axin* RNA and *nkd1* MO suppressed the decrease in the arc of *gsc* expression observed with *axin* alone (Figs. 8F,L) (*axin* RNA + *nkd1* MO = 58.8° ± 11.5, n=29; $p<0.05$). This confirms our previous observations that reducing Nkd function results in increased Wnt/β-catenin signaling. In contrast, our analysis at 2–3 somites in *slb* mutants had a different result. Injection of *axin* RNA alone had no effect on axial mesendoderm extension at 2–3 somites (Figs. 8H,M) (Uninj = 30.6% ± 14.8, n=22; *axin* RNA = 35.2% ± 12.7, n=30;

p=0.23). However, co-injection of *axin* RNA and *nkd1* MO into *slb* embryos resulted in a significant suppression of the axial mesendoderm extension defect, similar to *nkd1* MO injections alone (Figs. 8I,M) (*axin* RNA + *nkd1* MO = 44.0% ± 16.9, n=30; p<0.01). Interestingly, in the *axin* and *nkd1* MO co-injections, we also observed mild suppression of the convergence defect in the neural plate, which we did not observe previously in *nkd1* MO injections alone (Figs. 8N) (Uninj = 0.225 ± 0.059, n=22; *axin* RNA = 0.209 ± 0.069, n=30; *axin* RNA + *nkd1* MO = 0.168 ± 0.071, n=30; p<0.01). This data argues that Nkd1 is actively antagonizing non-canonical Wnt/PCP signaling.

DISCUSSION

Nkd1 expression recapitulates active Wnt signaling

Previous studies have shown that Nkd proteins act as inducible negative regulators of Wnt signaling (Wharton et al., 2001; Yan et al., 2001a; Zeng et al., 2000). We have found that zebrafish *nkd1* and *nkd2* exhibit different expression patterns with *nkd2* being maternal and ubiquitously expressed while *nkd1* is, for the most part, expressed after MBT and in regions recapitulating active canonical Wnt signaling (Dorsky et al., 2002). One interesting and dynamic domain of *nkd1* expression is in the dorsal axial mesendoderm in the early gastrula (Figs. 1E–H). At shield stage, *nkd1* expression is absent from the dorsal epiblast, but is expressed in the internalized hypoblast (Figs. 1E,F). Subsequently at 75% epiboly, *nkd1* expression is detected in both the dorsal epiblast and in the internalized hypoblast layer, but expression appears to be excluded from internalizing cells (Figs. 1G,H). The initial expression pattern of *nkd1* in the dorsal region at dome stage, and then the axial mesendoderm at shield stage and at 75% epiboly is highly reminiscent of *fzA* expression, which is also expressed in similar domains, but unlike *nkd1* expression, *fzA* expression is restricted to the dorsal mesendoderm (Nasevicius et al., 1998). During segmentation stages, *nkd1* is expressed in the presomitic mesoderm suggesting that, as in mouse presomitic mesoderm, *nkd1* expression may be part of the segmentation clock (Dequeant et al., 2006; Ishikawa et al., 2004). Finally, the expression patterns of *nkd1* and *nkd2* are consistent with studies in the mouse where *nkd1* and *nkd2* have overlapping expression patterns and *nkd1* appears to be expressed in domains where there is active Wnt signaling (Wharton et al., 2001). Supporting the whole-mount in situ data, the qRT-PCR data demonstrates that *nkd1* expression is quite low pre-MBT, but rises significantly post-MBT.

The expression pattern of *nkd1* overlaps, but is very different than the expression of the genes encoding secreted Wnt antagonists *dkk1* and secreted frizzled related proteins (*sfrps*). Initially, *dkk1* and *nkd1* genes appear to share overlapping domains of expression as both are expressed in the ventrolateral mesoderm margin as well as the organizer at shield stage. However, after this stage, their expression patterns diverge. At 75% epiboly, *dkk1* is restricted to the lateral edge of the axial mesendoderm and anterior notochord (Hashimoto et al., 2000; Shinya et al., 2000), which is complementary to the expression of *nkd1* within the axial mesendoderm. Of all the early *sfrp* expression patterns, *sfrp3* has an expression profile that overlaps somewhat with *nkd1*. Both have expression within the axial mesendoderm at approximately 75% epiboly; however, this is the only expression domain of *sfrp3* in the early gastrula (Tendeng and Houart, 2006). Together, these unique expression patterns likely reflect the differences in their transcriptional regulation, with *nkd1* expression being a consistent target of canonical Wnt/β-catenin signaling (see below).

Activation of the canonical Wnt/β-catenin signaling pathway through overexpression of constitutively active β-catenin induced robust expression of *nkd1* in the early embryo (Fig. 2B). Similarly, inhibiting the pathway by overexpression of Axin reduced *nkd1* expression (Fig. 2D). Further, our analysis in *boz* mutants supports our hypothesis that *nkd1* is a likely target of canonical Wnt/β-catenin signaling. As predicted, we found that *nkd1* expression levels

decreased in the absence of *boz*, a direct target of maternal Wnt/β-catenin at dome stage (Bellipanni et al., 2006;Shimizu et al., 2000), but increased when there was ectopic Wnt8 signaling in *boz* mutants during gastrulation at shield stage (Fekany-Lee et al., 2000). In mz*oep* mutants, we also found that *nkd1* expression was reduced in the region adjacent to the dorsal gastrula organizer. This is similar to the effect on *wnt8* expression in the absence of Nodal signaling in mz*oep* mutants, which lack dorsolateral mesoderm (Erter et al., 2001). Finally, analysis of the *nkd1* promoter regions in both zebrafish and mouse reveals multiple Tcf/Lef binding sites, while these sites could not be identified the *nkd2* promoter region (TVR, RJC unpublished data). Collectively, this data is consistent with *D. melanogaster nkd* data and mouse *nkd1* data, which argue that these genes are direct targets of canonical Wnt/β-catenin signaling (Wharton et al., 2001;Zeng et al., 2000). While we have demonstrated that *nkd1* expression is positively regulated by canonical Wnt/β-catenin signaling, further experiments are needed to test if *nkd1* is a direct target of canonical Wnt/β-catenin in zebrafish. One caveat to this model is the late onset of *nkd1* expression, relative to *boz* and *mkp3* expression, in blastula stage embryos. This suggests that *nkd1* expression is not a direct target of maternal Wnt/β-catenin but might be downstream of it, similar to *gsc* and *chd* expression (Fekany et al., 1999;Shimizu et al., 2000). As for *nkd2*, our data suggests that *nkd2* is unlikely to be regulated by canonical Wnt/β-catenin signaling during early developmental stages.

Nkds antagonize canonical Wnt/β-catenin signaling

In determining if Nkd1 and Nkd2a have functional differences, we found that in all of our overexpression assays Nkd1 and Nkd2a displayed nearly identical activity. However, our loss of function experiments using morpholino oligonucleotides demonstrated that Nkd2, but not Nkd1, is required for restricting the earliest maternal Wnt/β-catenin signaling. Accordingly, our in situ analysis showed that robust *nkd1* expression starts in the putative organizer only at dome stage, which is slightly later than *mkp3* expression (Tsang et al., 2004) or *boz* expression (Koos and Ho, 1998; Yamanaka et al., 1998). This suggests that *nkd1* expression is not a direct target of maternal β-catenin but might be downstream of it, similar to *gsc* or *chd* expression (Fekany et al., 1999; Shimizu et al., 2000). We speculate that maternal Wnt/β-catenin signaling induces the expression of *boz*, which in turn represses the expression of the *vent*, *vox* and *ved* genes, which themselves are repressors of *gsc* and *chd* (Kawahara et al., 2000; Melby et al., 2000; Melby et al., 1999; Ramel and Lekven, 2004; Shimizu et al., 2002) and potentially of *nkd1*, although this needs to be determined.

At late blastula stage, *nkd1* is expressed in the entire ventrolateral blastoderm margin of the embryo, likely reflecting a combination of maternal Wnt/β-catenin and zygotic Wnt8 signaling (Kelly et al., 1995). We found that reducing Nkd1 function resulted in a moderate expansion of *gsc* expression at 30% epiboly. We interpret this to mean that Nkd1 is also required for limiting the size of the organizer, at a stage later than Nkd2, but before the onset of significant mediolateral Wnt8 activity. However, when we co-injected *nkd1* and *nkd2* MOs and assayed for *gsc* expression at 50% epiboly, we were surprised to find that there was no significant difference compared to uninjected controls. This difference in *gsc* expression at different time points is potentially due to competing events (Bellipanni et al., 2006). At 30% epiboly, organizer induction by Wnt/β-catenin signaling is enhanced by reducing Nkd1 and Nkd2 activity. This results in an expansion of the *gsc* expression domain at 30% epiboly. Subsequently, ventrolateral Wnt8 signaling is also enhanced by reducing Nkd1 and Nkd2 activity. This results in a reduction of the expanded *gsc* expression at 50% epiboly. These two events likely cancel each other out, resulting in a normal *gsc* expression pattern.

To address whether Nkd1 or Nkd2 could inhibit Wnt8 signaling at physiological levels, we took advantage of the *boz* mutants which have ectopic dorsal *wnt8* expression during late blastula and early gastrula stages (Fekany-Lee et al., 2000). We found that both Nkd1 and

Nkd2a overexpression was sufficient to suppress the *boz* axial mesoderm deficiency suggesting that Nkds can also inhibit ectopic Wnt8 activity. Similar suppression of axial mesoderm deficiency in *boz* mutants was achieved by the overexpression of a dominant negative Wnt8 (Fekany-Lee et al., 2000) or the injection of *wnt8* MOs (Erter et al., 2001). In support of this, Nkd1 and Nkd2 could also inhibit the neural posteriorizing activity of ectopic Wnt8, as co-injection of *nkd1* or *nkd2a* RNA with *wnt8* RNA effectively reduced the eyeless phenotype caused by Wnt8 overexpression. Taken together, these several lines of evidence support the notion that Nkd1 and Nkd2 are acting at several stages of development in inhibiting canonical Wnt/β-catenin signaling. This is consistent with published reports on mouse Nkd1, mouse Nkd2 and *D. melanogaster* Nkd (Wharton et al., 2001; Yan et al., 2001a; Zeng et al., 2000).

The effect of Nkds is consistent with that of the Wnt antagonists such as the secreted Dkk1 protein. Overexpression of *dkk1* RNA results in an expansion of the organizer and *dkk1* can also effectively suppress the axial mesoderm deficiency in *boz* mutants (Hashimoto et al., 2000; Shinya et al., 2000). However, whereas they appear to be acting in similar ways, there are some significant differences. During gastrula stages *nkd1*, but not *dkk1*, recapitulates active canonical Wnt/β-catenin signaling (Hashimoto et al., 2000; Shinya et al., 2000). Dkk1 is a secreted Wnt antagonist and upon RNA injections, with doses as low as 5–20 pg, results in an anteriorized embryo, shortened anterior-posterior axis and a reduction of somites (Hashimoto et al., 2000; Shinya et al., 2000). In contrast, injections of *nkds'* RNA at 800 pg, and even as high as 2.4 ng, produced no obvious morphological phenotype. Yet clearly, Nkds are capable of antagonizing canonical Wnt/β-catenin signaling. It is likely that Nkds by themselves are ineffective Wnt antagonists, and they either require a limiting co-factor or they need to be activated. Whereas we have not identified a co-factor, there is support for the latter hypothesis from our co-injection experiments with *wnt8* RNA. Wnt8 has potent posteriorizing activity, but this activity is effectively inhibited by overexpressed Nkds, which by themselves do not produce an overt neural patterning phenotype. It is possible that Wnt8 activity, in addition to inducing *nkd1* expression, is activating Nkds, which then become potent inhibitors. A proposed model would be that an initiating Wnt signaling event would trigger the Wnt/β-catenin pathway invoking targeted gene transcription. One of the targets would be *nkd1*, which upon further Wnt activity, would become activated. This activated Nkd protein would then effectively block further signaling of the Wnt pathway. This model would provide tight, cell autonomous temporal control of the pathway. In contrast, secreted Wnt antagonists, such as SFRPs and Dkk, would provide cell autonomous and non-cell autonomous spatial and specificity control.

The mechanism of maternal canonical Wnt/β-catenin activation in dorsal axis specification remains controversial. One report argues that activation occurs at the level of β-catenin (Rowning et al., 1997) while another argues that it is at the level of Dishevelled (Dsh) (Miller et al., 1999). However, recent data argues that Wnt11 is the ligand responsible for the maternal signaling component (Tao et al., 2005). Our epistasis analysis argues that Nkds are functioning upstream of β-catenin but downstream of a Wnt signal in organizer formation. In agreement with this, several reports have now demonstrated that Nkds bind Dsh (Angers et al., 2006; Li et al., 2004; Rousset et al., 2001; Rousset et al., 2002; Wharton et al., 2001; Yan et al., 2001a). Therefore, our data supports the hypothesis that maternal Wnt/β-catenin activation is upstream of β-catenin; however, we can not distinguish whether it is at the level of Dsh or Wnts.

Nkds antagonize non-canonical Wnt/PCP signaling

The role of Nkds in non-canonical signaling is poorly understood and there is no PCP phenotype in the *D. melanogaster nkd* mutant (Zeng et al., 2000). Therefore, we aimed to determine if Nkd1 or Nkd2 can also affect non-canonical Wnt/PCP signaling. Using $slb^{tz216/tz216}$ mutants defective in Wnt11 signaling (Heisenberg et al., 2000), we found that overexpression of Nkd1

or Nkd2a exacerbated the *slb* gastrulation and cyclopia phenotypes. Conversely, reducing Nkd1 function partially suppressed the *slb* phenotype. Our further studies showed that suppression of the *slb* phenotype, in the presence of *nkd1* MO, is unlikely to be a result of inhibited canonical Wnt/β-catenin signaling. We demonstrate that inhibiting canonical signaling downstream of Nkds does not affect the ability of the *nkd1* MO to suppress the *slb* phenotype. While this is a novel phenotype for Nkd1, it is not entirely unprecedented. Recently, Dkk1 has been reported to positively affect C&E movements independent of its antagonistic affects on canonical Wnt/β-catenin signaling (Caneparo et al., 2007). Also, in the characterization of the *slb* phenotype, it was found that activation or inhibition of canonical Wnt/β-catenin had no effect on the *slb* phenotype (Heisenberg et al., 2000). Therefore, we argue that Nkd1 has the ability to antagonize non-canonical Wnt/PCP signaling independent of its antagonism of canonical Wnt/β-catenin signaling.

This result poses an interesting question. If *nkd1* expression is a target of canonical Wnt signaling, then how is Nkd1 perturbing non-canonical Wnt/PCP signaling? Further, if *nkd1* expression is exclusively regulated by canonical Wnt/β-catenin signaling, then the expression of *nkd1* in the axial mesendoderm at 75% epiboly suggests that there is active, or recently activated, canonical Wnt/β-catenin signaling in this domain. Further experiments will be required to understand the interactions between canonical and non-canonical Wnt signaling.

An endogenous role for Nkds in antagonizing PCP signaling has not been identified in *D. melanogaster*, arguing that Nkds may strictly function in canonical Wnt/β-catenin signaling. However, our data suggests that Nkds do indeed antagonize non-canonical Wnt/PCP signaling. This discrepancy between the two systems may be due to the fact that there is no known homologue to Wnt11 in *D. melanogaster* and indeed Wnt ligands have not been implicated in PCP signaling in flies. Further, vertebrate Nkd proteins, but not *D. melanogaster* Nkd, contain a myristoylation site that localizes Nkd to the membrane (Li et al., 2004). Therefore, it is plausible that a Wnt ligand may be required for proper functioning of vertebrate Nkds (see below).

Our observations that either the reduction or overexpression of Nkd2 exacerbates the *slb* phenotype is reminiscent of the effect of Trilobite/Van gogh-like-2 (Tri/Vangl2) on the *slb* phenotype (Jessen et al., 2002). Tri/Vangl2 is a transmembrane protein associated with non-canonical Wnt/PCP signaling in both vertebrates and flies (Jessen et al., 2002; Park and Moon, 2002; Taylor et al., 1998). Although Tri/Vangl2 and Wnt11 functionally interact, Tri/Vangl2 reduction or overexpression could not suppress the *slb* phenotype. In other assays, Tri/Vangl2 antagonized Wnt11 function (Jessen et al., 2002). This suggests that, similar to Tri/Vangl2, Nkd2 can modulate non-canonical Wnt/PCP signaling but it is not simply a positive or negative component of a linear Wnt/PCP pathway. Further experiments will be necessary to clarify the role of Nkd2 in non-canonical Wnt/PCP signaling and its relationship to canonical Wnt/β-catenin signaling.

In the model presented above for canonical Wnt/β-catenin signaling, we propose that Nkds need to be activated, potentially by a Wnt signal, in order to antagonize the pathway. If this model holds true for non-canonical Wnt/PCP signaling, then why is there a phenotype when Nkds are either overexpressed or reduced in *slb* mutants, which presumably have no Wnt11 signaling? This is likely due to Wnt5 signaling. Recent reports have established that Wnt5/*ppt* is partially redundant with Wnt11/*slb* in the extension of axial mesendoderm (Kilian et al., 2003; Westfall et al., 2003). This demonstrates that there is still some non-canonical Wnt/PCP signaling occurring in the axial mesendoderm in *slb* mutants via Wnt5. Therefore, according to our model, overexpression of Nkds can block the effect of endogenous Wnt5 in *slb* mutants, exacerbating the cyclopia and axial mesendoderm C&E phenotype. Congruent with this model,

reducing Nkd1 activity would allow recurrent signaling through Wnt5 in *slb* mutants, partially suppressing the axial C&E defect.

Finally, our results contrast somewhat with a previously published report in *X. laevis* that Nkd overexpression inhibits C&E by stimulating the non-canonical Wnt/PCP pathway (Yan et al., 2001a). Here, we argue that overexpression of Nkd inhibits C&E by blocking the non-canonical Wnt/PCP pathway. In support of this, we find that reducing Nkd1 function can suppress the axial migration defect in *slb* mutants, arguing that the pathway is being activated, in the absence of Nkd function. Our results may be unique to *slb* mutants or differences in assays and organisms employed, but they indicate that zebrafish Nkds function as inhibitors of both canonical and non-canonical Wnt signaling and not as a simple switch between these pathways.

Acknowledgments

We would like to thank members of the Solnica-Krezel and Coffey labs for support and valuable comments. We are grateful to Amy Bradshaw and Jared Ruddick for excellent fish care and Amy Bradshaw for help with the in vitro fertilizations. We are also grateful to Susan R. Opalenik, Ph.D. and the Vanderbilt Skin Diseases Research Center Molecular Genetics Core Laboratory for qRT-PCR. RJC acknowledges the support of NCI P50 95103 Special Program of Research Excellence (SPORE), U01 084239 Mouse Models of Human Cancers Consortium (MMHCC) and RO1 CA46413. Work in the LSK lab was supported by NIH RO1 GM55101.

References

Akimenko MA, Ekker M, Wegner J, Lin W, Westerfield M. Combinatorial expression of three zebrafish genes related to distal-less: part of a homeobox gene code for the head. J Neurosci 1994;14:3475–3486. [PubMed: 7911517]

Angers S, Thorpe CJ, Biechele TL, Goldenberg SJ, Zheng N, MacCoss MJ, Moon RT. The KLHL12-Cullin-3 ubiquitin ligase negatively regulates the Wnt-beta-catenin pathway by targeting Dishevelled for degradation. Nat Cell Biol 2006;8:348–357. [PubMed: 16547521]

Bellipanni G, Varga M, Maegawa S, Imai Y, Kelly C, Myers AP, Chu F, Talbot WS, Weinberg ES. Essential and opposing roles of zebrafish beta-catenins in the formation of dorsal axial structures and neurectoderm. Development 2006;133:1299–1309. [PubMed: 16510506]

Cadigan KM, Nusse R. Wnt signaling: a common theme in animal development. Genes Dev 1997;11:3286–3305. [PubMed: 9407023]

Caneparo L, Huang YL, Staudt N, Tada M, Ahrendt R, Kazanskaya O, Niehrs C, Houart C. Dickkopf-1 regulates gastrulation movements by coordinated modulation of Wnt/beta catenin and Wnt/PCP activities, through interaction with the Dally-like homolog Knypek. Genes Dev 2007;21:465–480. [PubMed: 17322405]

Chamorro MN, Schwartz DR, Vonica A, Brivanlou AH, Cho KR, Varmus HE. FGF-20 and DKK1 are transcriptional targets of beta-catenin and FGF-20 is implicated in cancer and development. Embo J 2005;24:73–84. [PubMed: 15592430]

Ciruna B, Jenny A, Lee D, Mlodzik M, Schier AF. Planar cell polarity signalling couples cell division and morphogenesis during neurulation. Nature 2006;439:220–224. [PubMed: 16407953]

Clevers H. Wnt/beta-catenin signaling in development and disease. Cell 2006;127:469–480. [PubMed: 17081971]

Dequeant ML, Glynn E, Gaudenz K, Wahl M, Chen J, Mushegian A, Pourquie O. A complex oscillating network of signaling genes underlies the mouse segmentation clock. Science 2006;314:1595–1598. [PubMed: 17095659]

Dorsky RI, Sheldahl LC, Moon RT. A transgenic Lef1/beta-catenin-dependent reporter is expressed in spatially restricted domains throughout zebrafish development. Dev Biol 2002;241:229–237. [PubMed: 11784107]

Erter CE, Wilm TP, Basler N, Wright CV, Solnica-Krezel L. Wnt8 is required in lateral mesendodermal precursors for neural posteriorization in vivo. Development 2001;128:3571–3583. [PubMed: 11566861]

Fekany K, Yamanaka Y, Leung T, Sirotkin HI, Topczewski J, Gates MA, Hibi M, Renucci A, Stemple D, Radbill A, Schier AF, Driever W, Hirano T, Talbot WS, Solnica-Krezel L. The zebrafish bozozok locus encodes Dharma, a homeodomain protein essential for induction of gastrula organizer and dorsoanterior embryonic structures. Development 1999;126:1427–1438. [PubMed: 10068636]

Fekany-Lee K, Gonzalez E, Miller-Bertoglio V, Solnica-Krezel L. The homeobox gene bozozok promotes anterior neuroectoderm formation in zebrafish through negative regulation of BMP2/4 and Wnt pathways. Development 2000;127:2333–2345. [PubMed: 10804176]

Giraldez AJ, Copley RR, Cohen SM. HSPG modification by the secreted enzyme Notum shapes the Wingless morphogen gradient. Dev Cell 2002;2:667–676. [PubMed: 12015973]

Gonzalez EM, Fekany-Lee K, Carmany-Rampey A, Erter C, Topczewski J, Wright CV, Solnica-Krezel L. Head and trunk in zebrafish arise via coinhibition of BMP signaling by bozozok and chordino. Genes Dev 2000;14:3087–3092. [PubMed: 11124801]

Gonzalez-Sancho JM, Aguilera O, Garcia JM, Pendas-Franco N, Pena C, Cal S, Garcia de Herreros A, Bonilla F, Munoz A. The Wnt antagonist DICKKOPF-1 gene is a downstream target of beta-catenin/TCF and is downregulated in human colon cancer. Oncogene 2005;24:1098–1103. [PubMed: 15592505]

Gritsman K, Zhang J, Cheng S, Heckscher E, Talbot WS, Schier AF. The EGF-CFC protein one-eyed pinhead is essential for nodal signaling. Cell 1999;97:121–132. [PubMed: 10199408]

Haddon C, Smithers L, Schneider-Maunoury S, Coche T, Henrique D, Lewis J. Multiple delta genes and lateral inhibition in zebrafish primary neurogenesis. Development 1998;125:359–370. [PubMed: 9425132]

Hashimoto H, Itoh M, Yamanaka Y, Yamashita S, Shimizu T, Solnica-Krezel L, Hibi M, Hirano T. Zebrafish Dkk1 functions in forebrain specification and axial mesendoderm formation. Dev Biol 2000;217:138–152. [PubMed: 10625541]

Heisenberg CP, Nusslein-Volhard C. The function of silberblick in the positioning of the eye anlage in the zebrafish embryo. Dev Biol 1997;184:85–94. [PubMed: 9142986]

Heisenberg CP, Tada M, Rauch GJ, Saude L, Concha ML, Geisler R, Stemple DL, Smith JC, Wilson SW. Silberblick/Wnt11 mediates convergent extension movements during zebrafish gastrulation. Nature 2000;405:76–81. [PubMed: 10811221]

Huelsken J, Behrens J. The Wnt signalling pathway. J Cell Sci 2002;115:3977–3978. [PubMed: 12356903]

Inohaya K, Yasumasu S, Araki K, Naruse K, Yamazaki K, Yasumasu I, Iuchi I, Yamagami K. Species-dependent migration of fish hatching gland cells that express astacin-like proteases in common [corrected]. Dev Growth Differ 1997;39:191–197. [PubMed: 9108332]

Ishikawa A, Kitajima S, Takahashi Y, Kokubo H, Kanno J, Inoue T, Saga Y. Mouse Nkd1, a Wnt antagonist, exhibits oscillatory gene expression in the PSM under the control of Notch signaling. Mech Dev 2004;121:1443–1453. [PubMed: 15511637]

Jessen, JR.; Solnica-Krezel, L. Morphogenetic cell movements shaping the zebrafish gastrula. In: Marek, M., editor. Advances in Developmental Biology and Biochemistry. Elsevier Press; 2005.

Jessen JR, Topczewski J, Bingham S, Sepich DS, Marlow F, Chandrasekhar A, Solnica-Krezel L. Zebrafish trilobite identifies new roles for Strabismus in gastrulation and neuronal movements. Nat Cell Biol 2002;4:610–615. [PubMed: 12105418]

Jho EH, Zhang T, Domon C, Joo CK, Freund JN, Costantini F. Wnt/beta-catenin/Tcf signaling induces the transcription of Axin2, a negative regulator of the signaling pathway. Mol Cell Biol 2002;22:1172–1183. [PubMed: 11809808]

Kawahara A, Wilm T, Solnica-Krezel L, Dawid IB. Antagonistic role of vega1 and bozozok/dharma homeobox genes in organizer formation. Proc Natl Acad Sci U S A 2000;97:12121–12126. [PubMed: 11050240]

Kelly C, Chin AJ, Leatherman JL, Kozlowski DJ, Weinberg ES. Maternally controlled (beta)-catenin-mediated signaling is required for organizer formation in the zebrafish. Development 2000;127:3899–3911. [PubMed: 10952888]

Kelly GM, Greenstein P, Erezyilmaz DF, Moon RT. Zebrafish wnt8 and wnt8b share a common activity but are involved in distinct developmental pathways. Development 1995;121:1787–1799. [PubMed: 7600994]

Kilian B, Mansukoski H, Barbosa FC, Ulrich F, Tada M, Heisenberg CP. Max Planck Institute of Molecular Cell, B., and Genetics, P. D. G. The role of Ppt/Wnt5 in regulating cell shape and movement during zebrafish gastrulation. Mechanisms of development 2003;120(4):467–476. [PubMed: 12676324]

Kimmel CB, Ballard WW, Kimmel SR, Ullmann B, Schilling TF. Stages of embryonic development of the zebrafish. Dev Dyn 1995;203:253–310. [PubMed: 8589427]

Kobayashi M, Toyama R, Takeda H, Dawid IB, Kawakami K. Overexpression of the forebrain-specific homeobox gene six3 induces rostral forebrain enlargement in zebrafish. Development 1998;125:2973–2982. [PubMed: 9655819]

Koos DS, Ho RK. The nieuwkoid gene characterizes and mediates a Nieuwkoop-center-like activity in the zebrafish. Curr Biol 1998;8:1199–1206. [PubMed: 9811602]

Lekven AC, Thorpe CJ, Waxman JS, Moon RT. Zebrafish wnt8 encodes two wnt8 proteins on a bicistronic transcript and is required for mesoderm and neurectoderm patterning. Dev Cell 2001;1:103–114. [PubMed: 11703928]

Li C, Franklin JL, Graves-Deal R, Jerome WG, Cao Z, Coffey RJ. Myristoylated Naked2 escorts transforming growth factor alpha to the basolateral plasma membrane of polarized epithelial cells. Proc Natl Acad Sci U S A 2004;101:5571–5576. [PubMed: 15064403]

Marlow F, Zwartkruis F, Malicki J, Neuhauss SC, Abbas L, Weaver M, Driever W, Solnica-Krezel L. Functional interactions of genes mediating convergent extension, knypek and trilobite, during the partitioning of the eye primordium in zebrafish. Dev Biol 1998;203:382–399. [PubMed: 9808788]

McEwen DG, Peifer M. Wnt signaling: the naked truth? Curr Biol 2001;11:R524–526. [PubMed: 11470426]

Melby AE, Beach C, Mullins M, Kimelman D. Patterning the early zebrafish by the opposing actions of bozozok and vox/vent. Dev Biol 2000;224:275–285. [PubMed: 10926766]

Melby AE, Clements WK, Kimelman D. Regulation of dorsal gene expression in Xenopus by the ventralizing homeodomain gene Vox. Dev Biol 1999;211:293–305. [PubMed: 10395789]

Miller JR, Rowning BA, Larabell CA, Yang-Snyder JA, Bates RL, Moon RT. Establishment of the dorsal-ventral axis in Xenopus embryos coincides with the dorsal enrichment of dishevelled that is dependent on cortical rotation. J Cell Biol 1999;146:427–437. [PubMed: 10427095]

Miller-Bertoglio VE, Fisher S, Sanchez A, Mullins MC, Halpern ME. Differential regulation of chordin expression domains in mutant zebrafish. Dev Biol 1997;192:537–550. [PubMed: 9441687]

Montcouquiol M, Crenshaw EB, Kelley MW. Noncanonical Wnt Signaling and Neural Polarity (1). Annu Rev Neurosci 2006;29:363–386. [PubMed: 16776590]

Moon RT, Kimelman D. From cortical rotation to organizer gene expression: toward a molecular explanation of axis specification in Xenopus. Bioessays 1998;20:536–545. [PubMed: 9723002]

Moon RT, Kohn AD, De Ferrari GV, Kaykas A. WNT and beta-catenin signalling: diseases and therapies. Nat Rev Genet 2004;5:691–701. [PubMed: 15372092]

Nasevicius A, Hyatt T, Kim H, Guttman J, Walsh E, Sumanas S, Wang Y, Ekker SC. Evidence for a frizzled-mediated wnt pathway required for zebrafish dorsal mesoderm formation. Development 1998;125:4283–4292. [PubMed: 9753682]

Niida A, Hiroko T, Kasai M, Furukawa Y, Nakamura Y, Suzuki Y, Sugano S, Akiyama T. DKK1, a negative regulator of Wnt signaling, is a target of the beta-catenin/TCF pathway. Oncogene 2004;23:8520–8526. [PubMed: 15378020]

Park M, Moon RT. The planar cell-polarity gene stbm regulates cell behaviour and cell fate in vertebrate embryos. Nat Cell Biol 2002;4:20–25. [PubMed: 11780127]

Park TJ, Gray RS, Sato A, Habas R, Wallingford JB. Subcellular localization and signaling properties of dishevelled in developing vertebrate embryos. Curr Biol 2005;15:1039–1044. [PubMed: 15936275]

Polakis P. Wnt signaling and cancer. Genes Dev 2000;14:1837–1851. [PubMed: 10921899]

Ramel MC, Lekven AC. Repression of the vertebrate organizer by Wnt8 is mediated by Vent and Vox. Development 2004;131:3991–4000. [PubMed: 15269175]

Rousset R, Mack JA, Wharton KA Jr, Axelrod JD, Cadigan KM, Fish MP, Nusse R, Scott MP. Naked cuticle targets dishevelled to antagonize Wnt signal transduction. Genes Dev 2001;15:658–671. [PubMed: 11274052]

Rousset R, Wharton KA Jr, Zimmermann G, Scott MP. Zinc-dependent interaction between dishevelled and the Drosophila Wnt antagonist naked cuticle. J Biol Chem 2002;277:49019–49026. [PubMed: 12354775]

Rowning BA, Wells J, Wu M, Gerhart JC, Moon RT, Larabell CA. Microtubule-mediated transport of organelles and localization of beta-catenin to the future dorsal side of Xenopus eggs. Proc Natl Acad Sci U S A 1997;94:1224–1229. [PubMed: 9037034]

Schmidt C, Otto A, Luke G, Valasek P, Otto WR, Patel K. Expression and regulation of Nkd-1, an intracellular component of Wnt signalling pathway in the chick embryo. Anat Embryol (Berl). 2006

Schulte-Merker S, Hammerschmidt M, Beuchle D, Cho KW, De Robertis EM, Nusslein-Volhard C. Expression of zebrafish goosecoid and no tail gene products in wild-type and mutant no tail embryos. Development 1994a;120:843–852. [PubMed: 7600961]

Schulte-Merker S, van Eeden FJ, Halpern ME, Kimmel CB, Nusslein-Volhard C. no tail (ntl) is the zebrafish homologue of the mouse T (Brachyury) gene. Development 1994b;120:1009–1015. [PubMed: 7600949]

Shimizu T, Yamanaka Y, Nojima H, Yabe T, Hibi M, Hirano T. A novel repressor-type homeobox gene, ved, is involved in dharma/bozozok-mediated dorsal organizer formation in zebrafish. Mech Dev 2002;118:125–138. [PubMed: 12351176]

Shimizu T, Yamanaka Y, Ryu SL, Hashimoto H, Yabe T, Hirata T, Bae YK, Hibi M, Hirano T. Cooperative roles of Bozozok/Dharma and Nodal-related proteins in the formation of the dorsal organizer in zebrafish. Mech Dev 2000;91:293–303. [PubMed: 10704853]

Shinya M, Eschbach C, Clark M, Lehrach H, Furutani-Seiki M. Zebrafish Dkk1, induced by the pre-MBT Wnt signaling, is secreted from the prechordal plate and patterns the anterior neural plate. Mech Dev 2000;98:3–17. [PubMed: 11044603]

Spiegelman VS, Slaga TJ, Pagano M, Minamoto T, Ronai Z, Fuchs SY. Wnt/beta-catenin signaling induces the expression and activity of betaTrCP ubiquitin ligase receptor. Mol Cell 2000;5:877–882. [PubMed: 10882123]

Stachel SE, Grunwald DJ, Myers PZ. Lithium perturbation and goosecoid expression identify a dorsal specification pathway in the pregastrula zebrafish. Development 1993;117:1261–1274. [PubMed: 8104775]

Tao Q, Yokota C, Puck H, Kofron M, Birsoy B, Yan D, Asashima M, Wylie CC, Lin X, Heasman J. Maternal wnt11 activates the canonical wnt signaling pathway required for axis formation in Xenopus embryos. Cell 2005;120:857–871. [PubMed: 15797385]

Taylor J, Abramova N, Charlton J, Adler PN. Van gogh. A new drosophila tissue polarity gene. Genetics 1998;150:199–210. [PubMed: 9725839]

Tendeng C, Houart C. Cloning and embryonic expression of five distinct sfrp genes in the zebrafish Danio rerio. Gene Expr Patterns 2006;6:761–771. [PubMed: 16504595]

Topczewski J, Sepich DS, Myers DC, Walker C, Amores A, Lele Z, Hammerschmidt M, Postlethwait J, Solnica-Krezel L. The zebrafish glypican knypek controls cell polarity during gastrulation movements of convergent extension. Dev Cell 2001;1:251–264. [PubMed: 11702784]

Tsang M, Maegawa S, Kiang A, Habas R, Weinberg E, Dawid IB. A role for MKP3 in axial patterning of the zebrafish embryo. Development 2004;131:2769–2779. [PubMed: 15142973]

Veeman MT, Axelrod JD, Moon RT. A second canon. Functions and mechanisms of beta-catenin-independent Wnt signaling. Dev Cell 2003;5:367–377. [PubMed: 12967557]

Westerfield, M. The Zebrafish Book. A guide for the laboratory use of zebrafish (Brachydanio rerio). University of Oregon Press; 1995.

Westfall TA, Brimeyer R, Twedt J, Gladon J, Olberding A, Furutani-Seiki M, Slusarski DC. Wnt-5/pipetail functions in vertebrate axis formation as a negative regulator of Wnt/beta-catenin activity. J Cell Biol 2003;162:889–898. [PubMed: 12952939]

Wharton KA Jr, Zimmermann G, Rousset R, Scott MP. Vertebrate proteins related to Drosophila Naked Cuticle bind Dishevelled and antagonize Wnt signaling. Dev Biol 2001;234:93–106. [PubMed: 11356022]

Wodarz A, Nusse R. Mechanisms of Wnt signaling in development. Annu Rev Cell Dev Biol 1998;14:59–88. [PubMed: 9891778]

Yamanaka Y, Mizuno T, Sasai Y, Kishi M, Takeda H, Kim CH, Hibi M, Hirano T. A novel homeobox gene, dharma, can induce the organizer in a non-cell-autonomous manner. Genes Dev 1998;12:2345–2353. [PubMed: 9694799]

Yan D, Wallingford JB, Sun TQ, Nelson AM, Sakanaka C, Reinhard C, Harland RM, Fantl WJ, Williams LT. Cell autonomous regulation of multiple Dishevelled-dependent pathways by mammalian Nkd. Proc Natl Acad Sci U S A 2001a;98:3802–3807. [PubMed: 11274398]

Yan D, Wiesmann M, Rohan M, Chan V, Jefferson AB, Guo L, Sakamoto D, Caothien RH, Fuller JH, Reinhard C, Garcia PD, Randazzo FM, Escobedo J, Fantl WJ, Williams LT. Elevated expression of axin2 and hnkd mRNA provides evidence that Wnt/beta -catenin signaling is activated in human colon tumors. Proc Natl Acad Sci U S A 2001b;98:14973–14978. [PubMed: 11752446]

Yost C, Torres M, Miller JR, Huang E, Kimelman D, Moon RT. The axis-inducing activity, stability, and subcellular distribution of beta-catenin is regulated in Xenopus embryos by glycogen synthase kinase 3. Genes Dev 1996;10:1443–1454. [PubMed: 8666229]

Zeng W, Wharton KA Jr, Mack JA, Wang K, Gadbaw M, Suyama K, Klein PS, Scott MP. naked cuticle encodes an inducible antagonist of Wnt signalling. Nature 2000;403:789–795. [PubMed: 10693810]

Zeng YA, Verheyen EM. Nemo is an inducible antagonist of Wingless signaling during Drosophila wing development. Development 2004;131:2911–2920. [PubMed: 15169756]

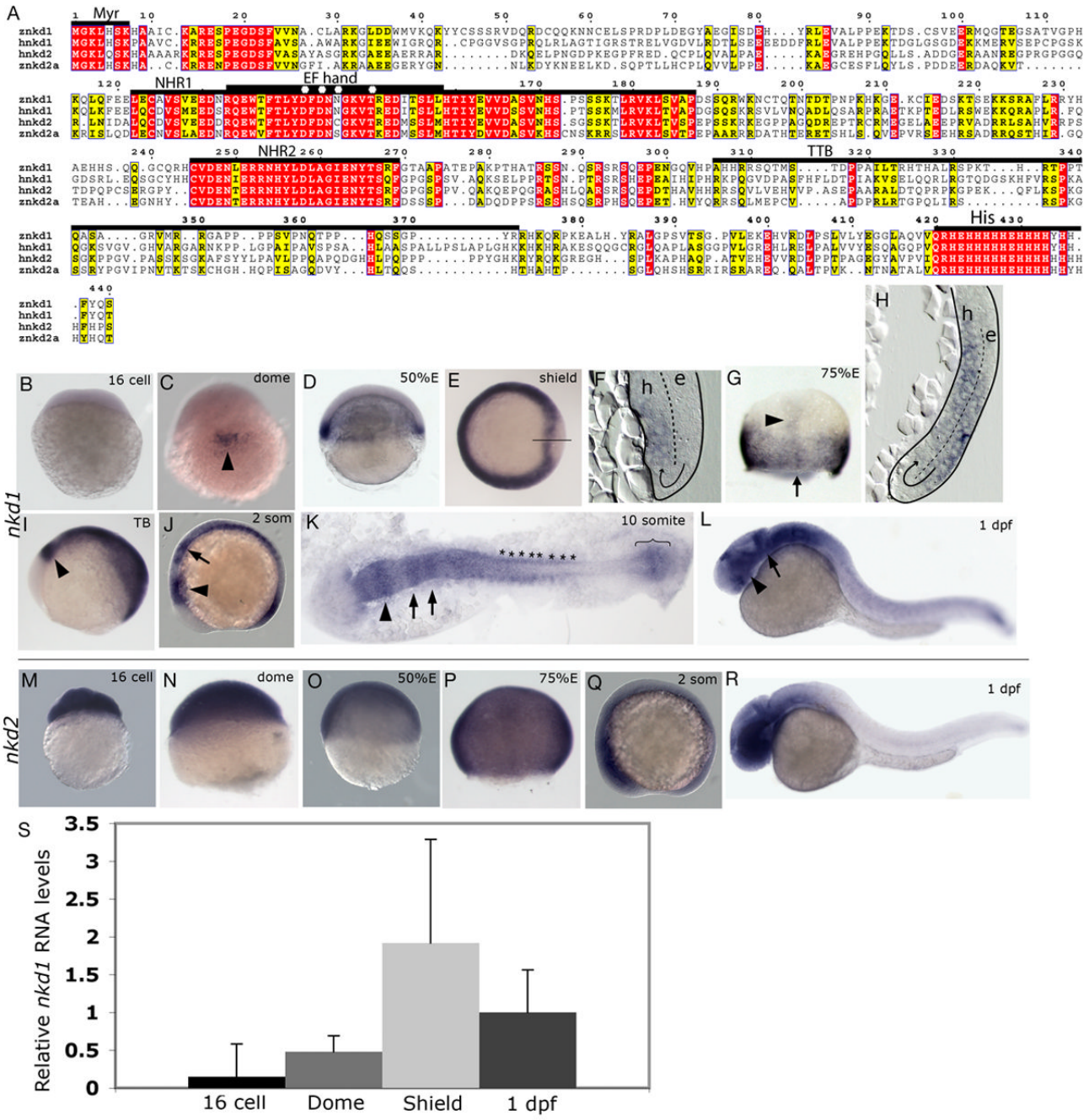

Fig. 1.

Alignment and expression of zebrafish *nkd1* and *nkd2*. (A) Alignment of zebrafish Nkd1 and Nkd2a amino acid sequence with human Nkd1 and Nkd2. Red boxes identify identical residues, while yellow boxes identify similarities. Numbering refers to the amino acid sequence of zebrafish Nkd1. Overlying bars define the different conserved domains. Myr, myristoylation sequence; NHR1, naked homology region 1; EF hand, identifies the homologous region in *D. melanogaster* Nkd that is predicted to bind zinc. The zinc-binding residues are denoted with an asterisks according to Zeng et al., (Zeng et al., 2000); NHR2, naked homology region 2; TTB, TGFα tail binding domain that is found in human Nkd2 (Li et al., 2004); His, Histidine rich domain. (B–L) Whole-mount in situ hybridization analysis of *nkd1* expression. (B) *nkd1*

expression is not detected in 16 cell stage, Pre-MBT embryos. (C) Expression of *nkd1* is detected in the presumptive organizer region (arrowhead) at dome stage. (D) At 50% epiboly, *nkd1* expression is in the entire blastoderm margin and by shield stage is reduced in the shield (E), only to be turned on in the axial mesendoderm (F). The solid line through the shield marks the plane of section shown in (F). In (F and H), the dashed line demarcates the ectodermal epiblast (e) and the mesendodermal hypoblast (h) layers and the arrow depicts route of cell movements during internalization. (G) At 75–80% epiboly, expression is observed in the margin and in the axial mesendoderm (arrowhead). The arrow identifies the plane of section in (H). (I) Tailbud (TB) stage. Mid-hindbrain boundary (mhb) is identified with an arrowhead. (J) In early somitogenesis, arrowhead identifies the mhb and the arrow is pointing to segmented expression in the hindbrain. (K) 10 somite stage, expression is observed in the mhb (arrowhead), hindbrain (arrows), developing somites (*) and in the presomitic mesoderm (bracket). (L) At 1dpf, expression continues in the mhb (arrow) but is now also observed in the developing eye (arrowhead). (M–R) Whole-mount in situ analysis of *nkd2* expression. (M–Q) *nkd2* expression is ubiquitous. At 1dpf, expression is confined to the anterior CNS and the posterior tail. (M) 16 cell stage; (N) dome stage; (O) 50% epiboly; (P) 75–80% epiboly; (Q) early somitogenesis stage; (R) 1 dpf. (S) Relative RNA levels determined by qRT-PCR for *nkd1*. Levels are normalized to 1 dpf (16 cell = 0.15 ± 0.43; Dome = 0.48 ± 0.21; Shield = 1.92 ± 1.37; 1 dpf = 1 ± 0.56). Error bars represent standard deviation. (B,M,N) lateral view, animal pole is to the top; (C,G,N,P) dorsal view, animal pole to the top; (D,O) lateral view, dorsal is to the right, animal pole to the top; (E) animal pole view, dorsal is to the right; (I,J,L,Q,R) lateral view, anterior is to the left; (K) flat mount view, anterior is the to the left. (F,H) sagital sections through regions identified in (E, line) and (G, arrow).

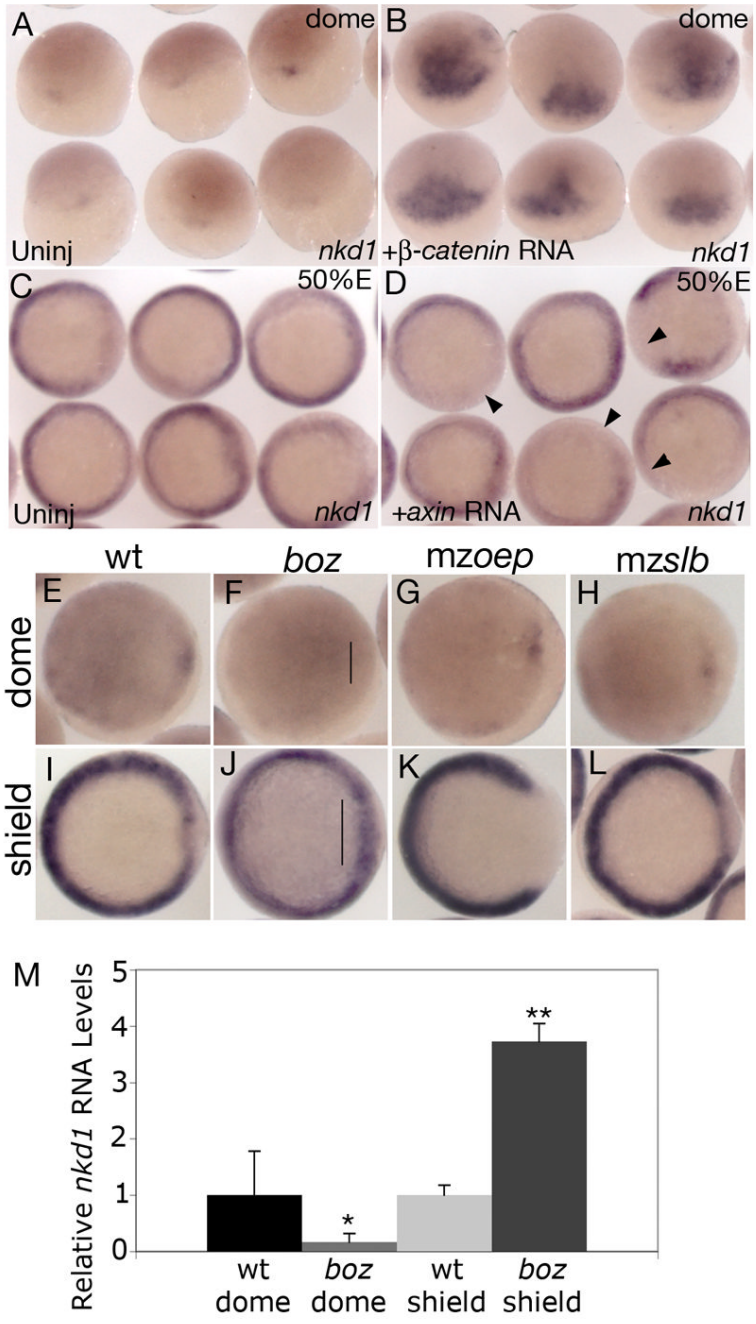

Fig. 2.

Nkd1 is a target of canonical Wnt/β-catenin signaling. Overexpression of constitutively active *β-catenin* RNA results in ectopic expression of *nkd1* at dome stage (B) compared to uninjected controls (A). Overexpression of *axin* RNA reduces endogenous *nkd1* expression in the mediolateral margin at 50% epiboly (D) compared to uninjected controls (C). Arrowheads point to domains of reduced or absent *nkd1* expression. (E–L) Expression of *nkd1* at dome stage (E–H) and shield stage (I–L) in wild-type (E,I) and different mutant backgrounds: (F,J) *boz*^{m168}, (G,K) maternal zygotic *one-eyed pinhead (*mz*oep*^{tz57}*)* and (H,L) maternal zygotic *silberblick (*mz*slb*^{tz215}). Note lack of *nkd1* expression at dome stage in *boz* mutants (bracket in F), but an increase in expression in the dorsal region at shield stage (bracket in J). (A,B)

dorsal view, animal pole is to the top. (C,D) Animal view. (E–L) Animal view, dorsal is to the right. While there is no change in *nkd1* expression at dome stage in mz*oep* (G), there is a dramatic reduction in *nkd1* expression in the dorsal region at shield stage (K). There is no observable difference in *nkd1* expression in mz*slb* compared to wild-type (H,L). (M) Relative qRT-PCR values for *nkd1* in wild-type and *boz* embryos at dome and shield stage. Values are normalized to wild-type for both dome and shield stage (wt dome = 1 ± 0.78; *boz* dome = 0.17 ± 0.15; wt shield = 1 ± 0.18; *boz* shield = 3.73 ± 0.32). Error bars represent standard deviation. (Students t-test, *, $p < 0.01$; **, $p < 0.001$).

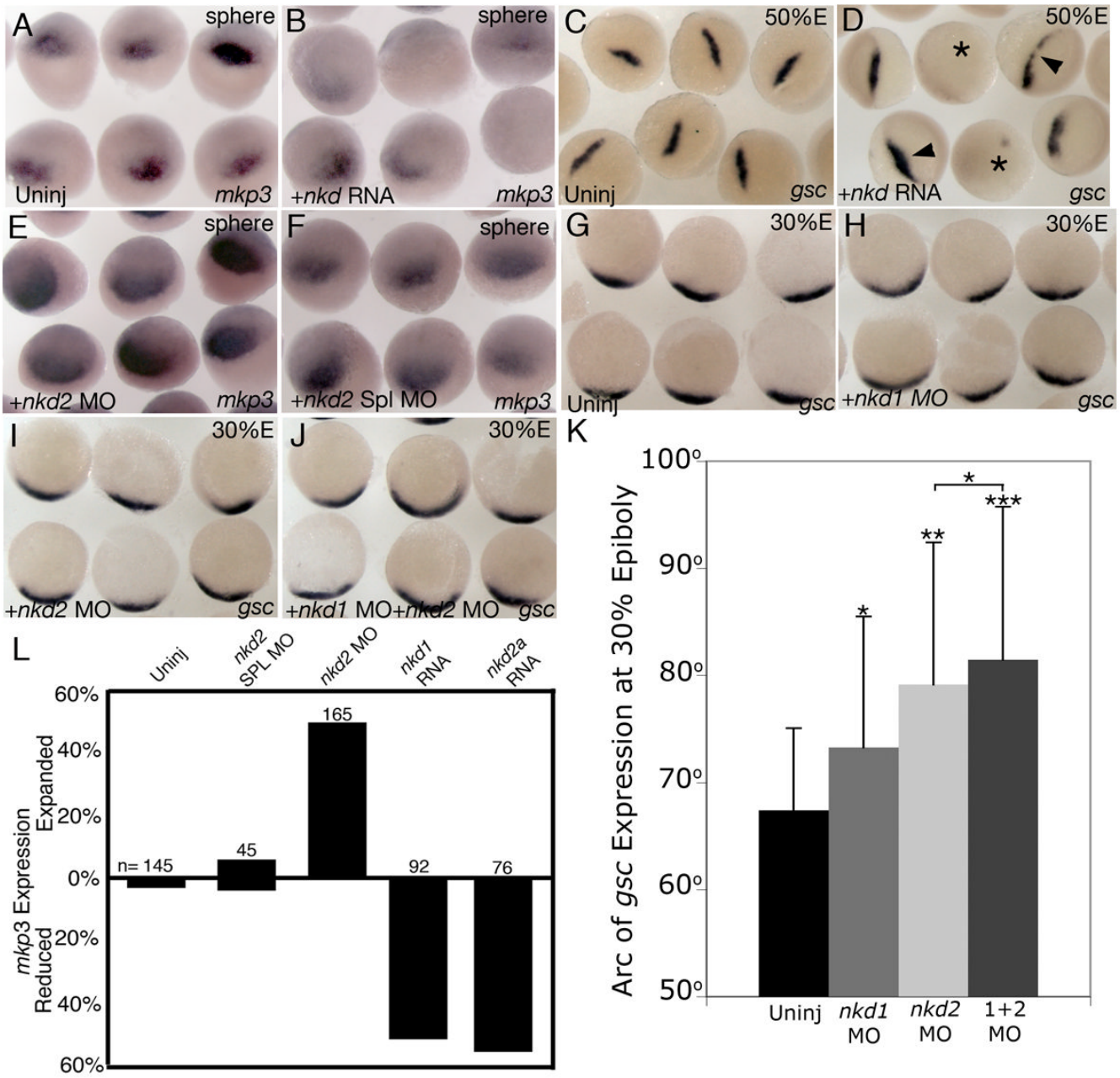

Fig. 3.

Nkds inhibit early canonical Wnt/β-catenin signaling. (B) *nkd1* or *nkd2a* injected within 7 min of fertilization and assayed at sphere stage for *mkp3* expression. (A) uninjected siblings. (D) Injection of either *nkd1* or *nkd2a* within 7 min of fertilization and assayed at 50% epiboly for *gsc* expression. Arrowheads identify embryos with expanded *gsc* expression and an asterisk identifies embryos with a decrease in *gsc* expression. (C) uninjected siblings. (E) Injection of *nkd2* MO at 1–2 cell stage and assayed at sphere stage for *mkp3* expression. (F) *nkd2* splice site MO control. This data is quantified in (L). (H) *nkd1* MO injected at the 1–2 cell stage and assayed at 30% epiboly for *gsc* expression. (G) uninjected siblings. (I) *nkd2* MO injected embryos at 1–2 cell stage and assayed for *gsc* expression at 30% epiboly. (J) A combination of *nkd1* MO and *nkd2* MOs were injected at the 1–2 cell stage and assayed at 30% epiboly for

gsc expression. (K) A graph of the arc of *gsc* expression at 30% epiboly under different conditions. Error bars represent standard deviation. (Students t-test, *, $p < 0.05$; **, $p < 0.001$; ***, $p<0.0001$). n= number of injected embryos. (A–F) dorsal view; G–J) animal view, dorsal is down).

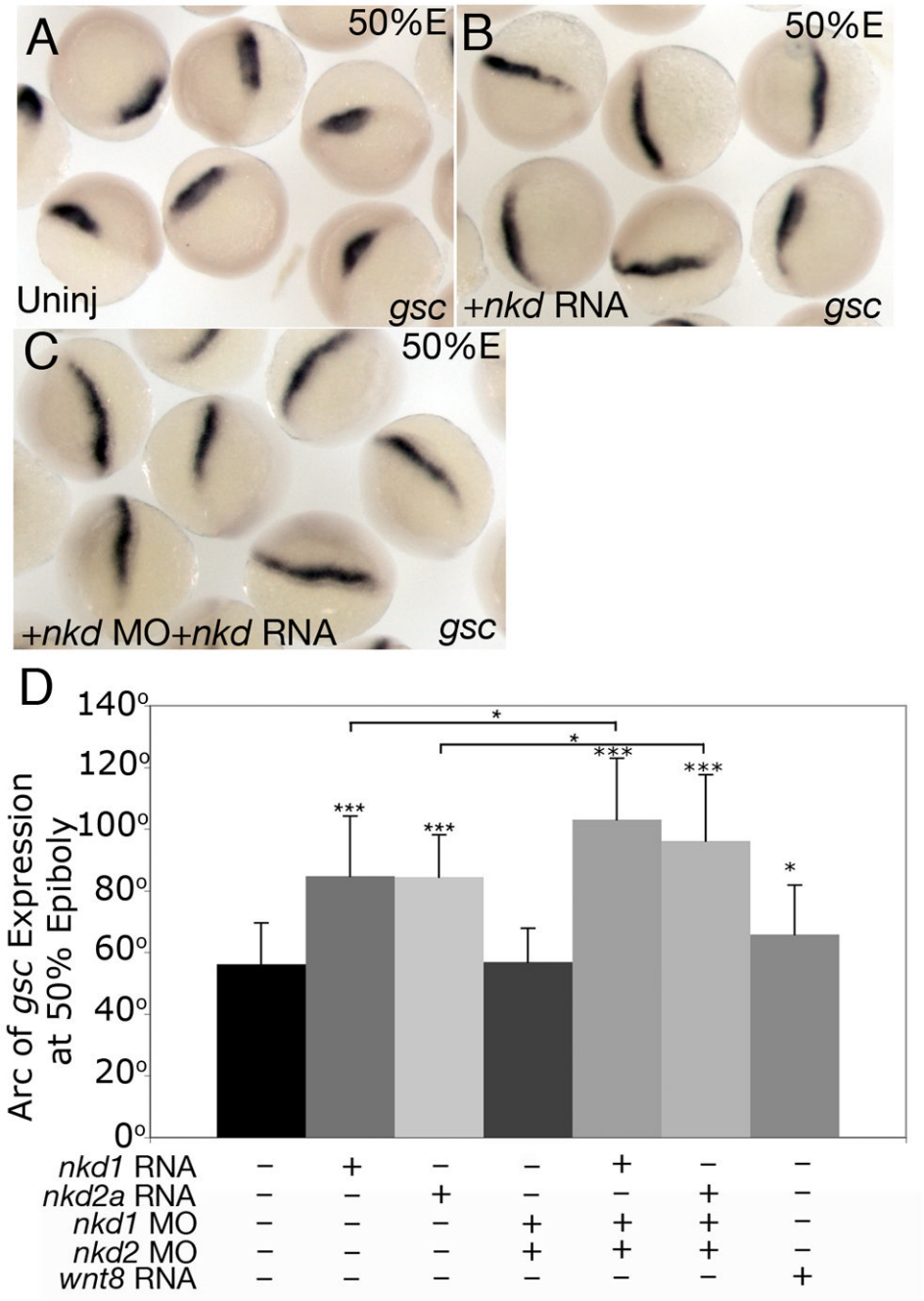

Fig. 4.

Nkds inhibit late canonical Wnt/β-catenin signaling. (A,B) Standard 1 to 2 cell overexpression of *nkd1 or nkd2a* RNA significantly expands *gsc* expression at 50% epiboly (B) compared with uninjected control siblings (A). (C) Injection of *nkd1* MO, *nkd2* MO and *nkd1* or *nkd2a* RNA that is insensitive to the MOs results in an even larger expansion of *gsc* expression at 50%. (A,B,C) dorsal view. This data is quantified in (D). Error bars represent standard deviation. (Students t-test, *, $p < 0.05$; ***, $p<0.0001$).

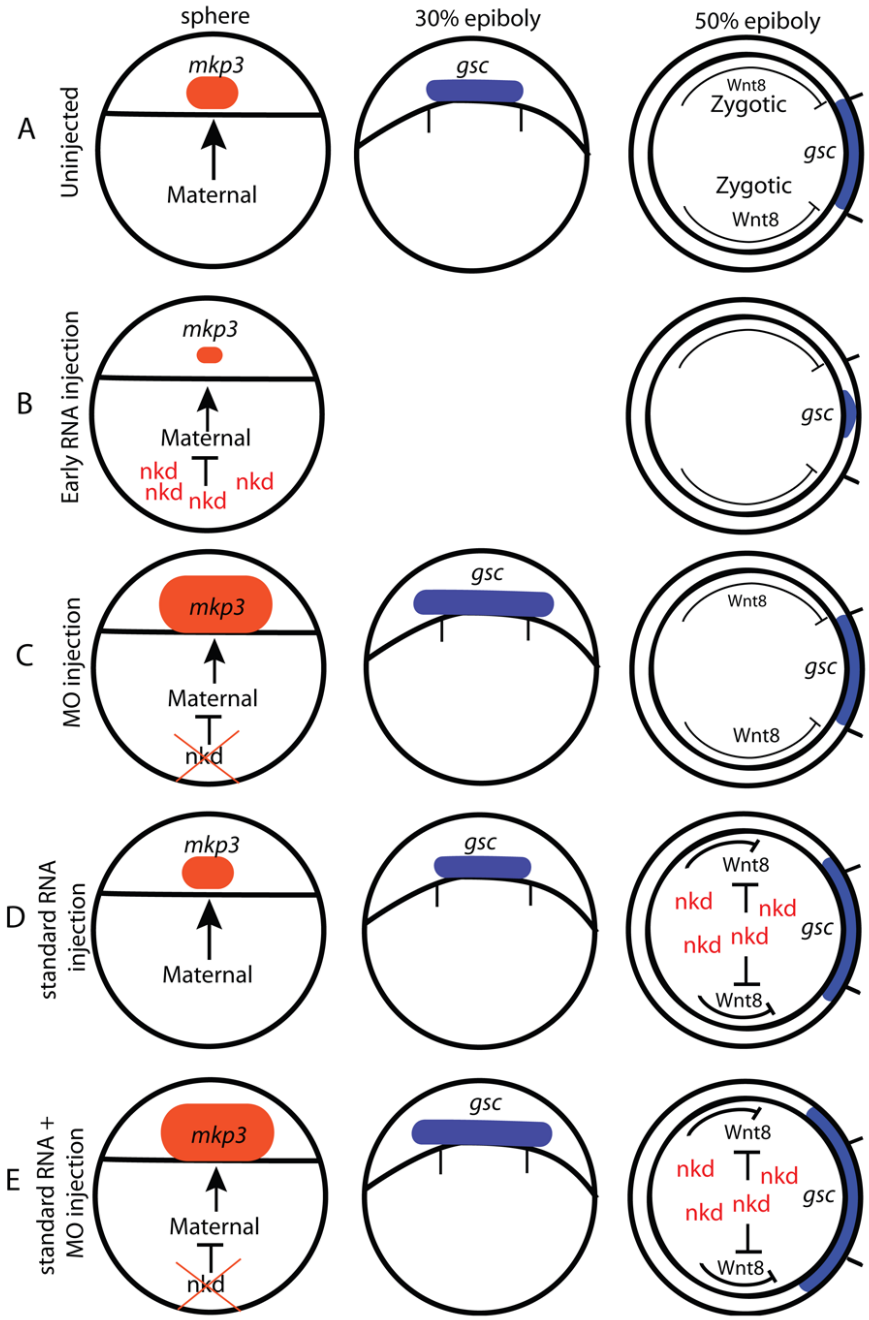

Fig. 5.

A summary of the regulation of canonical Wnt/β-catenin signaling by Nkd1 and Nkd2. (A) The arc of *gsc* expression at 50% epiboly is a result of both the positive and negative influences of canonical Wnt/β-catenin signaling. (B) Inhibiting maternal canonical Wnt/β-catenin signaling results in a reduction in *mkp3* expression at sphere stage and *gsc* expression at 50% epiboly. (C) Reducing Nkd2 function expands the size of *mkp3* expression at sphere stage. Reducing Nkd1 and Nkd2 function expands the arc of *gsc* expression at 30% epiboly, but there is no observable effect at 50% epiboly, likely due to an increase in ventrolateral Wnt8 signaling. (D) Inhibiting zygotic canonical Wnt/β-catenin signaling by Nkd1 or Nkd2 increases the arc of *gsc* expression at 50% epiboly. (E) The combined effects of *nkd1* and *nkd2* MO plus MO

insensitive *nkd1* or *nkd2a* RNA in a standard injection. The *nkd* MOs act early to increase the size of the organizer, while the RNA acts later to inhibit ventrolateral Wnt8 signaling. This results in a dramatic increase in the arc of *gsc* expression at 50% epiboly. Sphere and 30% epiboly stages are dorsal views, animal to the top; 50% epiboly stage, animal view, dorsal is to the right. Tick marks underneath the *gsc* expression domain at 30% epiboly and on the dorsal side of 50% epiboly stage diagrams represents the size of the wild-type *gsc* expression domain.

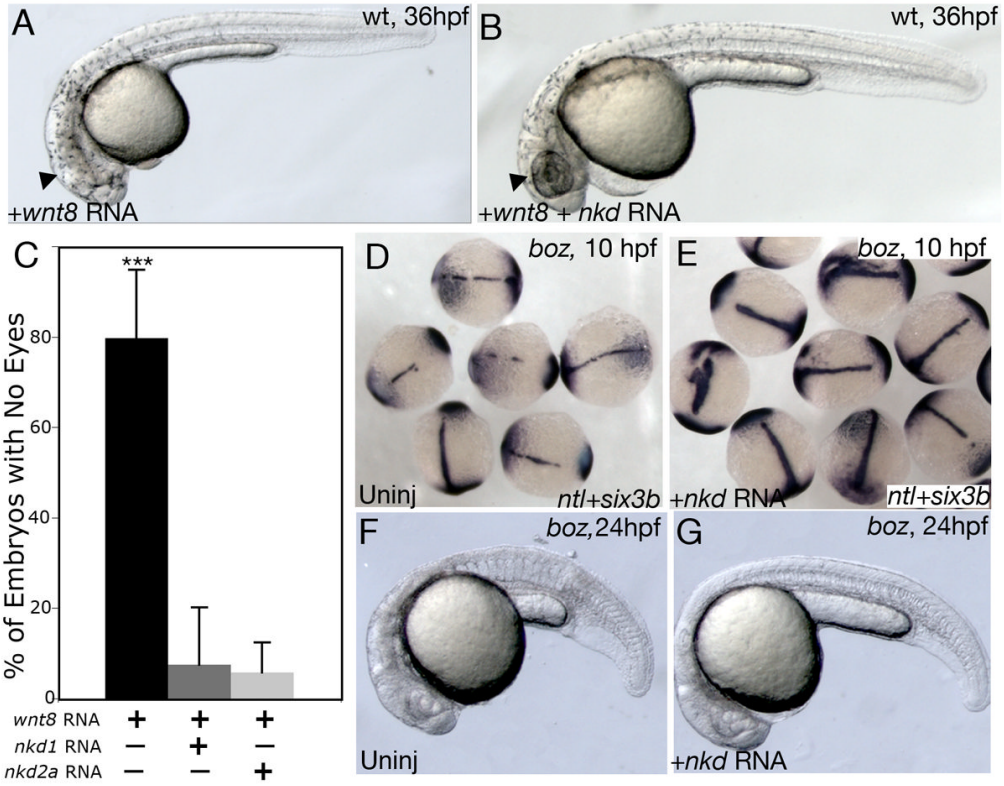

Fig. 6.

Nkds can antagonize ectopic Wnt8. (A) Overexpression of Wnt8 in wild-type (wt) embryos results in an eyeless phenotype. (B) Co-expression of *wnt8* and *nkd1* or *nkd2* results in a near complete suppression of the Wnt8 effect. This is quantified in (C). (D–G) *boz* mutants have ectopic Wnt8 activity in the dorsal mesoderm, which results in a reduction of axial tissue as demonstrated by reduced *ntl* expression (D), or in the physical absence of a notochord (F). The presumptive neuroectoderm is labeled with *six3b* which is also reduced in *boz* mutants (D). Injection of *nkd1* or *nkd2a* into *boz* embryos suppresses the deficiency of *ntl* expression in the notochord (E) and of a notochord at 24 hpf (G). Error bars represent standard deviation. (Students t-test; ***, $p<0.0001$). (A,B,F,G) lateral view, anterior to the left; (D,E) dorsal view.

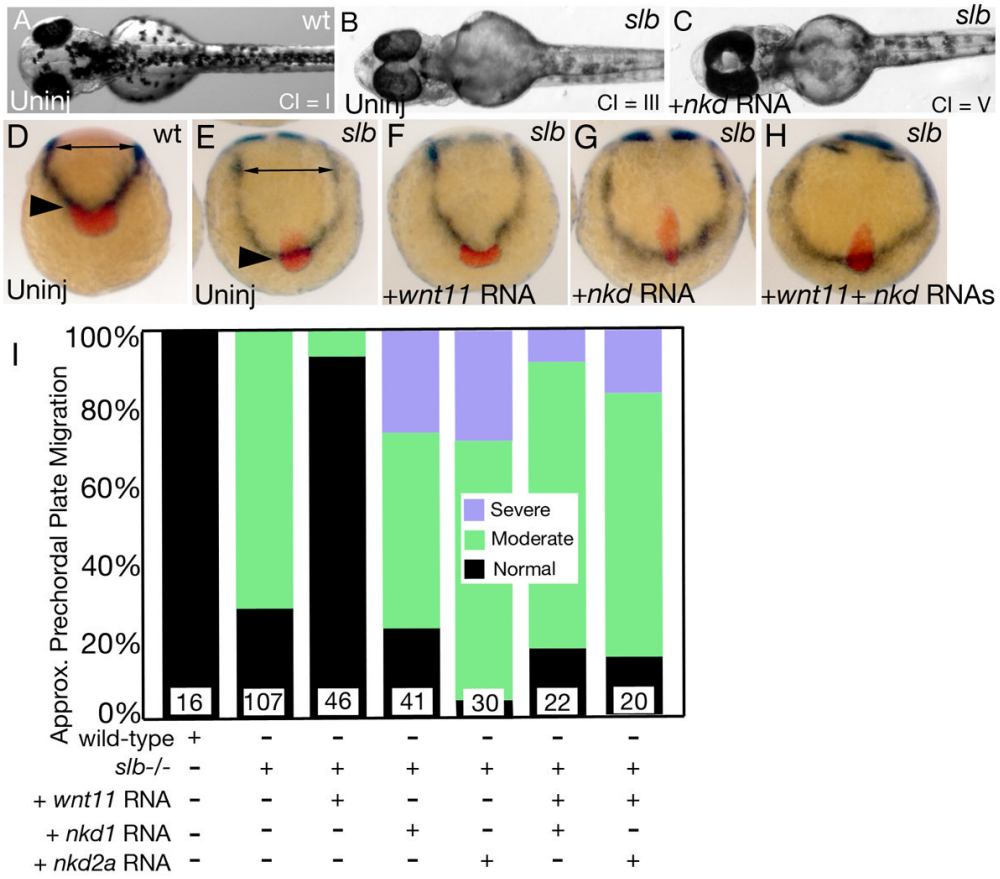

Fig. 7.

Nkds inhibit non-canonical Wnt/PCP signaling. (A) Wild-type embryos have a cyclopia index (CI) of 1, while *slb* mutants have a CI of 2.80 ± 0.46 (B). (C) *slb* embryos injected with *nkd1* or *nkd2a* RNA have an increase in cyclopia with a CI of 3.77 and 3.08 respectively. See text for details. (D–I) Analysis of prechordal plate position. (D) Wild-type embryos have a narrow neural plate (double headed arrow) and a prechordal plate that has fully extended past the neuroectoderm and non-neural ectoderm boundary (black arrowhead). (E) *slb* mutant embryos exhibit a wider neural plate due to impaired C&E (double headed arrow) and reduced extension of the axial mesendoderm (black arrowhead). (F) Injection of *wnt11* RNA into *slb* embryos can rescue the C&E defects in *slb* embryos. (G) Overexpression of *nkd1* or *nkd2a* RNA in *slb* embryos exacerbates the axial mesendoderm extension defect. (H) Co-expression of *wnt11* with *nkd1* or *nkd2a* results in a phenotype that resembles the *nkd* overexpression phenotype arguing that Nkds can block Wnt11 signaling. This data is semi-quantified in (I) where moderate is defined as ≤ ~50% of the *hgg* expression domain is within the *dlx3* expression domain and severe is defined as > ~50% of the *hgg* expression domain is within the *dlx3* domain. (A–C) 2 dpf, (A) dorsal view, (B,C) ventral views. (D–H) 2–3 somites, anterior view, dorsal is to the top, prechordal plate marked by *hgg* (red), neuroectoderm-non neural ectoderm boundary marked by *dlx3* (dark purple), developing somites (out of view) marked by *dlC* for staging confirmation.

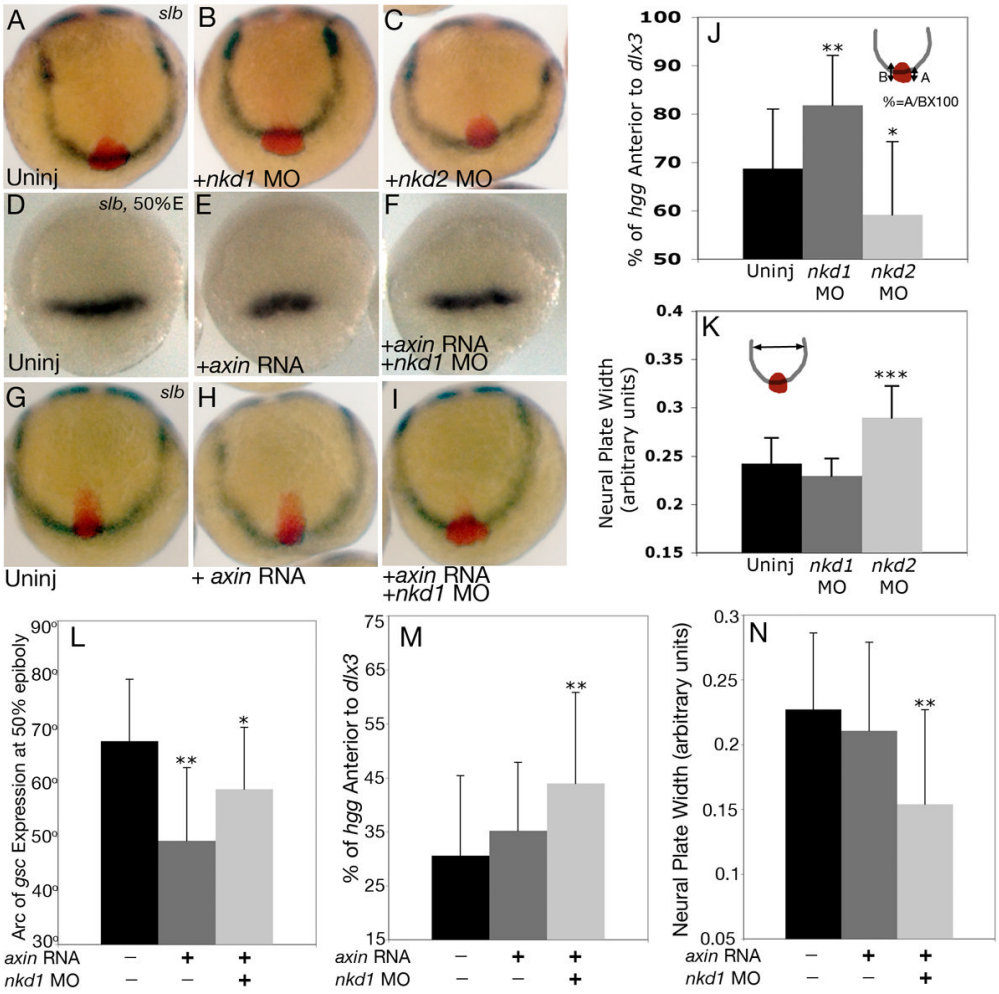

Fig. 8.

Reduction of Nkd1 can suppress the axial C&E defect in *slb*. (A) Uninjected *slb* mutant. (B) *slb* embryo injected with *nkd1* MO results in a suppression of the axial C&E defect observed in uninjected *slb* embryos, which is quantified in (J). Note that the convergence of the neural plate remains unchanged (K). In contrast, injection of *nkd2* MO exacerbates both the axial C&E (C,J) and the neural plate convergence phenotype in *slb* mutants (C,K). (D–F) dorsal view, animal pole to the top of *gsc* expression at 50% epiboly in *slb* mutants which are uninjected (D), injected with *axin* RNA (E) or *axin* RNA and *nkd1* MO (F). The arc of *gsc* expression is quantified in (L). (G–I) *slb* embryos from the same clutch as (D–F) analyzed for percent of axial extension. Anterior view, dorsal to the top of uninjected (G), *axin* RNA injected (H) and *axin* RNA and *nkd1* MO injected embryos (I). The percentage of axial extension is quantified in (M) and the width of the neural plate is quantified in (N). (A–C, G–I) 2–3 somite stage. The percentage of complete axial extension is calculated by measuring the proportion of total *hgg* expression that is over and past the *dlx3* expression domain. One Hundred percent would be defined as complete extension, as observed, for example, in wild-type (Fig. 7D). Markers are as described in Fig. 7. Error bars represent standard deviation. (Students t-test, *, $p < 0.05$; **, $p<0.01$; ***, $p<0.0001$).